CrossMark

The impact of revised simplified Arakawa–Schubert convection parameterization scheme in CFSv2 on the simulation of the Indian summer monsoon

**Malay Ganai · P. Mukhopadhyay ·
R. Phani Murali Krishna · M. Mahakur**

Abstract   Keeping the systematic bias of the climate forecast system model version 2 (CFSv2) in mind, an attempt is made to improve the Indian summer monsoon (ISM) rainfall variability in the model from diurnal through daily to seasonal scale. Experiments with default simplified Arakawa–Schubert (SAS) and a revised SAS schemes are carried out to make 15 years climate run (free run) to evaluate the model fidelity with revised SAS as compared to default SAS. It is clearly seen that the revised SAS is able to reduce some of the biases of CFSv2 with default SAS. Improvement is seen in the annual seasonal cycle, onset and withdrawal but most importantly the rainfall probability distribution function (PDF) has improved significantly. To understand the reason behind the PDF improvement, the diurnal rainfall simulation is analysed and it is found that the PDF of diurnal rainfall has significantly improved with respect to even a high resolution CFSv2 T382 version. In the diurnal run with revised SAS, the PDF of rainfall over central India has remarkably improved. The improvement of diurnal cycle of total rainfall has actually been contributed by the improvement of diurnal cycle of convection and associated convective rainfall. This is reflected in outgoing longwave radiation and high cloud diurnal cycle. This improvement of convective cycle has resolved a long standing problem of dry bias by CFSv2 over Indian land mass and wet bias over equatorial Indian Ocean. Besides the improvement, there are some areas where there are still scopes for further development. The cold tropospheric temperature bias, low cloud fractions need further improvement. To check the role of shallow convection, another free run is made with revised SAS along with shallow convection (SC). The major difference between the new and old SC schemes lies in the heating and cooling behavior in lower-atmospheric layers above the planetary boundary layer. However, the inclusion of revised SC scheme could not show much improvement as compared to revised SAS with deep convection. Thus, it seems that revised SAS with deep convection can be a potentially better parameterization scheme for CFSv2 in simulating ISM rainfall variability.

Keywords   Revised SAS · Indian summer monsoon · CFSv2 · Rainfall

1 Introduction

The skillful prediction of Indian summer monsoon rainfall (ISMR) plays a pivotal role in deciding the socioeconomic growth of the country (Gadgil and Gadgil 2006). The Indian summer monsoon (ISM) which prevails from June through September (JJAS) shows great amount of spatial and temporal variability (Goswami 2005; Hoyos and Webster 2007). The extreme departure (±1.5 standard deviation of the mean) from normal rainfall (droughts and floods) severely affects agricultural output and consequently the economy of India (Mooley and Parthasarathy 1984; Webster et al. 1998; Kripalani et al. 2003; Chaudhari et al. 2010). Therefore, understanding the spatio-temporal variabilities of the summer monsoon and improving its simulation and prediction at various space and time scale has immense importance.

Despite a substantial improvement in model skill in recent times (Kim et al. 2012; Lee et al. 2013), the

M. Ganai · P. Mukhopadhyay (✉) · R. P. M. Krishna · M. Mahakur
Indian Institute of Tropical Meteorology, Dr. Homi Bhabha Road, Pashan, Pune 411008, Maharashtra, India
e-mail: parthasarathi64@gmail.com; mpartha@tropmet.res.in

latest generation of atmospheric general circulation models (GCMs) still has serious difficulties in simulating monthly or seasonal precipitation (Wang et al. 2008). It has been well established (Webster et al. 1998) that ISM is a fully coupled land–atmosphere–ocean climate system and hence it should be better reproduced by coupled ocean–land–atmosphere GCMs (CGCMs). Several studies (Fennessy et al. 1994; Sperber and Palmer 1996; Goswami 1998; Gadgil and Sajani 1998; Sabre et al. 2000, etc.) attempt to simulate ISM circulation features and monsoon variability using atmospheric general circulation model (AGCM). However, they concluded that the simulation were poor for the ISMR. Waliser et al. (2003) show that the AGCM fails to reproduce the eastward propagating convection and the northwest-southeast-tilted rainband associated with the Boreal Summer Intraseasonal Oscillations (BSISOs). By evaluating ECHAM5 AGCM simulation, Abhik et al. (2014) concluded that the model reasonably reproduces the seasonal mean-state of the atmosphere during ISM. However, they found some notable discrepancies in the simulated summer mean moisture and rainfall distribution. Several intercomparison projects have also been carried out to explore the skill of the ocean–atmosphere coupled models. The major conclusion shows that the models are able to broadly capture the large scale mean features (spatio-temporal distributions of rainfall, wind circulations etc.) of the monsoon (Krishna Kumar 2005; Wang et al. 2004, 2008; Kim et al. 2008; Kug et al. 2008; Lee et al. 2010). However, the simulation of proper spatio-temporal structure of intraseasonal variabilities remains a challenging task (Waliser et al. 2003; Lin et al. 2008; Sperber and Annamalai 2008). Recently, the National Center for Environmental Prediction (NCEP) Climate Forecast System (CFS) model (a CGCM) is being adopted in India under a National Monsoon Mission Programme of Ministry of Earth Sciences, for predicting seasonal and intraseasonal monsoon rainfall. Number of studies using NCEP CFS version 1 (CFSv1) have shown reasonable skill in reproducing the seasonal and intraseasonal variabilities of the ISM (Yang et al. 2008; Pattanaik and Kumar 2010; Lee Drbohlav and Krishnamurthy 2010; Chaudhari et al. 2013; Suhas et al. 2013; Abhilash et al. 2014). However, certain systematic biases remained to be resolved. It may be worthy to mention that Lin et al. (2008) reported, most of the models overestimate the near-equatorial precipitation, underestimate the variability of the northward propagating Intraseasonal oscillation and westward propagating 12–24 day mode by analyzing ocean–atmosphere CGCM participating in the Fourth Assessment Report (AR4) of intergovernmental panel on climate change (IPCC). Sperber and Annamalai (2008) indicate that the lack of the eastward propagating convection across the Maritime Continents, is one of the major biases causing the unusual tilting of the rainband in CGCMs. It has already been reported (Kang et al. 2002; Wang et al. 2005; Pattnaik et al. 2013) that monsoon prediction/simulation is determined by ocean–atmosphere coupling, model resolution and also by the model physics (Slingo et al. 1996; Inness et al. 2001; Kemball-Cook et al. 2002; Zhang and Mu 2005; Zhang et al. 2006). By analyzing 20 years of CFSv1 and CFS version 2 (CFSv2) simulations of ISM, Saha et al. (2014) showed that the spatial pattern of seasonal mean rainfall, wind circulations, rainfall variance and northward propagation of intraseasonal oscillation (ISO) are more realistic in CFSv2 as compared to CFSv1. The difference between CFSv2 and CFSv1 lies in the fact (Saha et al. 2014) that CFSv2 incorporates advanced parameterization schemes. It also has improved atmospheric and ocean model (Modular Ocean Model version 3 (MOM3) in CFSv1 and MOM version 4 (MOM4) in CFSv2) with higher horizontal resolution. CFSv2 utilizes four layer Noah land-surface model, whereas CFSv1 has two layer land-surface model. In spite of improved model physics and horizontal resolution, Saha et al. (2014) also reported that the dry bias of monsoon rainfall over Indian land mass is more prominent in CFSv2. Sharmila et al. (2013) reported that monsoon intraseasonal oscillation (MISO) simulated by CFSv2 has more realistic northward propagation than its atmosphere-only counterpart which is the NCEP global forecast system (GFS) model. Recently, Goswami et al. (2014) attempted to find out possible explanation for the dry precipitation bias over the Indian landmass in the CFSv2 simulated mean monsoon. They revealed that the synoptic variance simulated by CFSv2 is significantly lower than its ISO variance over many regions across the globe and particularly over Indian land mass as compared to TRMM. They indicate possible deficiency in the convective parameterization scheme of CFSv2. Another recent study by Ajayamohan et al. (2014) highlights the importance of a new "multicloud model parameterization" in simulating Asian Monsoon ISO on an aquaplanet GCM. The analysis demonstrates the role of multicloud model parameterization in successfully simualting westward propagating of Rossby wave like disturbances and northward propagation of MISO.

Although some of the above studies (Saha et al. 2014; Chaudhari et al. 2013; Sharmila et al. 2013; Goswami et al. 2014) efficiently identified the systematic biases in mean rainfall simulation of the ISM, improvement towards resolving those biases is yet to be achieved. Increasing only the resolution in CFS does not bring much success (Saha et al. 2014; Sahai et al. 2014) especially in terms of dry bias over Indian land mass and wet bias over equatorial Indian Ocean (EIO). This indicates that there is possibly a need for improvement in the model physics to improve some of the above mentioned biases of the ISM. So far in all the earlier studies (Pokhrel et al. 2012; Saha et al. 2014; Chaudhari et al. 2013; Goswami et al. 2014, etc.), the ISM simulations

are done using the default SAS available with CFS. In the present study, we have used a revised version of simplified Arakawa–Schubert (SAS) deep convection parameterization (DCP) scheme in CFSv2 at T126 (spectral model at Triangular truncation 126–110 km) following Han and Pan (2011). In the revised DCP scheme, the cumulus convection is made stronger and deeper to deplete more instability in the atmospheric column and result in the suppression of the excessive grid-scale precipitation. The stronger and deeper convection is made through larger cloud-base mass flux and higher cloud tops which appear to effectively eliminate the remaining instability in the atmospheric column. Whereas, the old SAS deep convection scheme does not fully eliminate the instability and consequently an explicit convective ascent occurs at the grid scale, producing unrealistically heavy precipitation. Han and Pan (2011) also revised the shallow convection (SC) scheme by employing a mass flux parameterization which produces heating throughout the convection layers replacing the old turbulent diffusion based approach. By analyzing 1-month CFSv2 run at T126 horizontal resolution with revised SC and DCP schemes in SAS, Han and Pan (2011) demonstrated its advantages in reducing biases of low cloud cover, temperature, global 500 hPa geopotential height etc. They have also showed an improvement in forecast of Hurricane tracks over Atlantic and Eastern Pacific. However, in the present study, we have mainly focused on the application of revised DCP scheme along with old SC scheme in CFSv2 simulation of ISMR. Although, much improvement was reported by Han and Pan (2011), what remains to be seen is whether the revised SAS with DCP scheme could resolve some of the noted biases of CFSv2 over Indian monsoon domain.

Keeping the above issues in mind, we have attempted to find out how far the revised DCP can improve some of the existing biases particularly related to rainfall over Indian monsoon region in CFSv2. As the diurnal rainfall plays an important role in deciding the daily rainfall, we would like to analyze the impact of revised DCP on diurnal rainfall through daily to seasonal rainfall distribution of ISM. This study in one hand would show the robustness of the scheme in its application over Indian monsoon rainfall and may also help the forecaster in improving the skill of forecast using CFSv2. Along with revised SAS with DCP scheme; we intend to analyze the impact of revised SC in CFSv2 in simulating ISMR. Thereby, a brief analysis of precipitation and convective rainfall has been provided at the end of Sect. 3.

2 Model description, data used and methodology

NCEP CFSv2 (Saha et al. 2013) is the latest version of fully coupled land–atmosphere–ocean model with advanced physics, increased resolution and refined initialization to improve the seasonal climate forecasts. The GFS model consists of a spectral resolution of T126 (~100 km) with 64 hybrid vertical levels. The oceanic component is the Geophysical Fluid Dynamics Laboratory (GFDL) Modular Ocean Model, version 4p0d (Griffies et al. 2004) at 0.25°–0.5° grid spacing with 40 vertical layers. CFSv2 has a 3-layer interactive (2 layers of sea-ice and 1 layer of snow) global sea ice model, as well as a global land data assimilation system. It has a 4-level Noah land surface model (Ek et al. 2003) with interactive vegetation. CFSv2 uses a prognostic cloud parameterization scheme by Zhao and Carr (1997). The default convection scheme used in GFS is the simplified Arakawa–Schubert (SAS) convection with momentum mixing. The revised SAS deep convection parameterization scheme is implemented based on the study by Han and Pan (2011). Major differences from the old SAS deep convection scheme (Pan and Wu 1995) are described in details in Han and Pan (2011). In this study, we have performed two free runs each for 15 years of CFSv2-T126, one with default/old SAS convection scheme and another with revised SAS scheme with the same initial condition and the output is stored for every 24 h. The term "free run" indicates that the coupled model is run freely without any external inputs except for solar forcing and initial conditions. To study the diurnal variability of ISM, we also executed three free runs and output stored for every 3 h each for 5 years, one with old SAS and another with revised SAS scheme for CFSv2-T126 and the last one is with old SAS but for CFSv2-T382 (~38 km). These runs were carried out on the Prithvi High Performance Computing system (IBM P6-575) at Indian Institute of Tropical Meteorology (IITM), Pune, India. The atmosphere and the ocean initial conditions are taken from NCEP Climate Forecast System Reanalysis (CFSR; Saha et al. 2010).

Various observations and reanalysis products are utilized to evaluate the model simulation. The simulated precipitation over the Indian land-points is validated using gridded 0.5° × 0.5° daily rainfall dataset for the year 1991–2005 from India Meteorological Department (IMD, Rajeevan and Bhate 2008). Daily Tropical Rainfall Measuring Mission (TRMM) 3B42 version 7 (V7) gridded precipitation data (Huffman et al. 2007) at a horizontal resolution of 0.25° × 0.25° for the year 1998–2012 is used. The National Oceanic and Atmospheric Administration (NOAA) Outgoing Longwave Radiation (OLR) daily data set from 1998 to 2012 (Liebmann and Smith 1996) is analyzed to examine the convective variability. Daily air temperature data is taken from NCEP reanalysis (Kalnay et al. 1996) for the period 1998–2012. Convective component of daily rainfall from TRMM 3G68 data set (1998–2008) at 0.5° × 0.5° horizontal resolutions is examined. It is a combination of various TRMM products-2A12, 2A25 and 2B31 (Haddad

et al. 1997a, b; Iguchi et al. 2000; Kummerow et al. 2001). Additionally, the diurnal rainfall simulation is validated by using 5 years (1999–2003) of 3 hourly TRMM V7 rainfall data sets for JJAS. To examine the diurnal variability of OLR over Indian monsoon region, we have utilized 3 hourly OLR data from Kalpana-1 very high resolution radiometer (VHRR) satellite observations (Mahakur et al. 2013) for the period 2005–2012 for JJAS. Finally, International Satellite Cloud Climatology Project (ISCCP) data (Schiffer and Rossow 1983) which is available for the period July 1983–December 2009 have been utilized in this study. Cloud parameters are estimated by combining data from several geostationary and polar orbiting satellites to prepare a long period of cloud climatology. Calibrated radiances are used for validating parameterized clouds in climate model and for improved understanding of radiation budget and hydrological cycle. We have used the ISCCP D2 datasets (monthly means), which is an improved version from earlier C series in terms of radiance calibration, cloud detection and radiative transfer modeling (Rossow and Schiffer 1999). The cloud classification employs visible, near-infrared and infrared (IR) channels during day time whereas full diurnal scale data is available from IR based algorithm only. Hence, we used cloud types data estimated only from IR channel. ISCCP classifies clouds as low [cloud top pressure (PC) >680 hPa] and high (PC ≤ 440 hPa) from IR based PC obtained from estimated cloud top temperature and TIROS (Television Infrared Observation Satellite) operational vertical sounder temperature profile retrieved in seven layers. On the other hand, CFSv2 designates clouds as low (PC > 642 hPa) and high (PC ≤ 350 hPa) below 45° latitude. Above 45 latitude, CFSv2 defines clouds as low (PC > 750 hPa) and high (PC ≤ 500 hPa). Although, the definition of low and high clouds in ISCCP and in CFSv2 is not exactly similar, we can get a qualitative picture of the parameters through comparison.

The smoothed climatology of rainfall for all the data sets is prepared based on the annual mean and first three harmonics of the long-term mean seasonal cycle. The calculation for the intraseasonal variability is based on 10–90 day band pass filtered (Duchon 1979) daily anomalies computed by subtracting daily smoothed climatology for all the datasets from the observation and the model simulations.

3 Results and discussions

3.1 Simulation of JJAS precipitation and OLR climatology

In order to identify model fidelity in simulating mean JJAS precipitation, we have shown the impact of revised SAS with deep convection parameterization (DCP) scheme on CFSv2 in Fig. 1a–c. It is clear from Fig. 1a–c that the large scale mean precipitation features are captured by CFSv2 with both SAS schemes. However, the positive precipitation bias over the equatorial Pacific and west coast of Africa in CFSv2 with old SAS simulations has reduced in revised SAS (Fig. 1b, c). This is further reflected in Fig. 1d, e, which shows the difference between model and observation. The improvement in revised SAS over old SAS in CFSv2 can be better visualized in Fig. 1f. From the global (50°S–50°N) mean, root mean square error (RMSE) and pattern correlation coefficient (CC) values, revised SAS may seem equivalent to old SAS but the improvement in the distribution of rainfall over the major precipitation centres are noteworthy in revised SAS simulation. The JJAS mean distribution of OLR is shown in Fig. 2a–c. Both models appear to overestimate OLR over southern Indian Ocean, eastern pacific and over Indian landmass regions. However, relative improvement of revised SAS over old SAS simulation can be seen over western pacific (Fig. 2e) and Indian landmass region (Fig. 2f). Global mean and RMSE values appear to be marginally improved in the revised SAS scheme.

The JJAS precipitation climatology appears to be remarkably improved over the Indian region (Fig. 3a–c) which is the domain of focus in this study. The observed and simulated JJAS mean rainfall (mm day^{-1}) over the ISM region is shown in Fig. 3. The precipitation maxima are observed over the Western Ghats (WG), northeast India and eastern shore and northern part of Bay of Bengal (BoB) in TRMM (Fig. 3a). The model with old SAS convection parameterization scheme (Fig. 3b) appears to underestimate the precipitation amount substantially over central Indian region and overestimate over equatorial Indian Ocean (EIO) region. Similar rainfall biases are also reported by earlier studies (Pokhrel et al. 2012; Saha et al. 2014; Chaudhari et al. 2013; Sharmila et al. 2013; Goswami et al. 2014). The model simulation with old SAS also underestimates the precipitation over northern part of BoB as shown in Fig. 3b. These rainfall biases over central India (CI), EIO and northern part of BoB are found to substantially improve in CFSv2 with revised SAS convection parameterization scheme as shown in Fig. 3c. The rainfall amount over CI and northern BoB has significantly increased compared to Fig. 3b whereas over EIO it agrees well with the observation. To get quantitatively better picture of model simulated rainfall biases, we have evaluated the model-bias (with respect to TRMM) as shown in Fig. 3d–f. Figure 3d depicts that rainfall bias in CFSv2 with old SAS scheme over central India is around −4 to −2 mm day^{-1} and over EIO it is around 2 to 4 mm day^{-1}. These biases are almost completely removed in the revised version of SAS scheme as depicted in Fig. 3e. However, in some pockets over ISM region, underestimation of
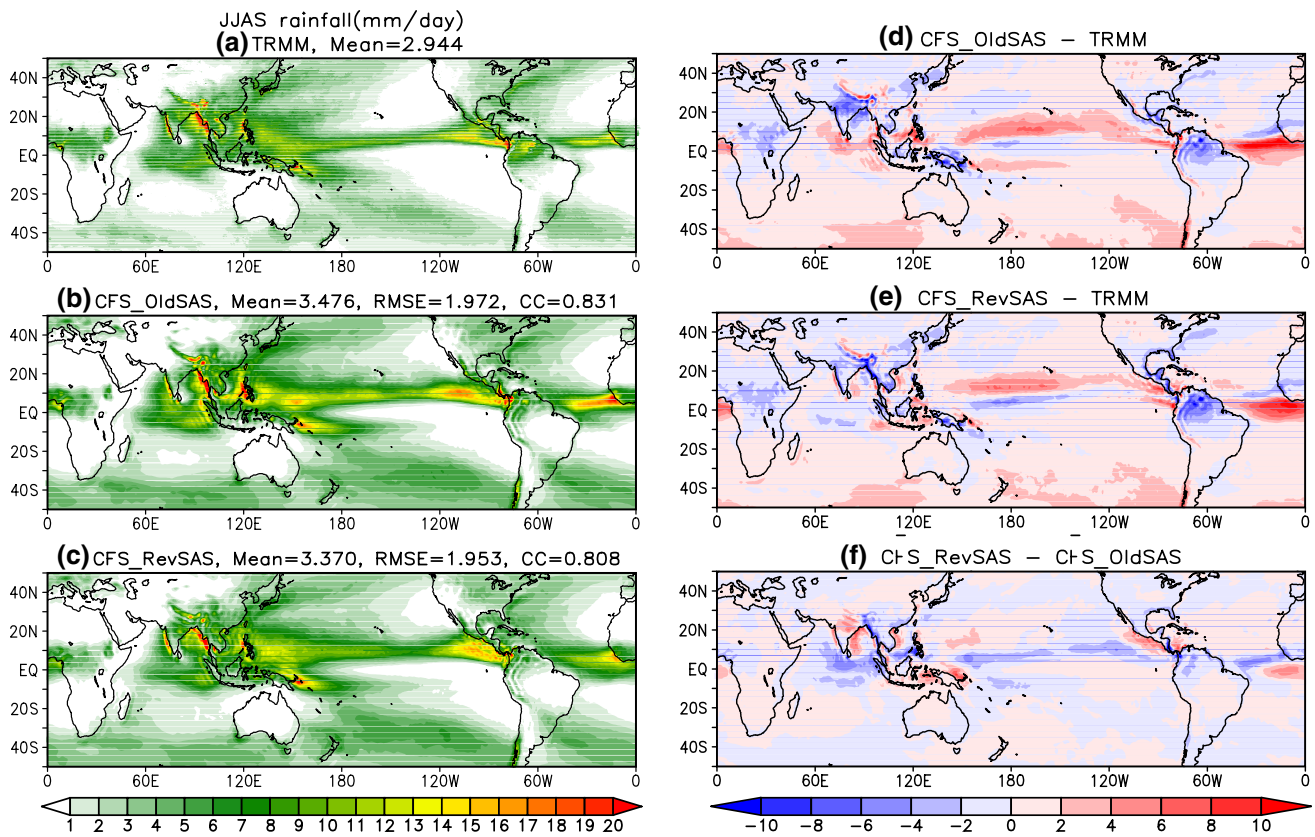
Fig. 1 JJAS mean climatological precipitation (mm day^{-1}) over global domain (50°N–50°S) from **a** TRMM, CFSv2 with **b** old SAS and **c** revised SAS scheme. Biases (mm day^{-1}) in CFSv2 with **d** old SAS and **e** revised SAS scheme with respect to TRMM and **f** biases in CFSv2 with revised SAS with respect to old SAS scheme. Global mean rainfall values are calculated for both observation and models (Fig. 1a–c). RMSE and pattern CC is calculated for old SAS (Fig. 1b) and revised SAS (Fig. 1c) with respect to TRMM

precipitation can be seen (Fig. 3b). Figure 3c represents performance of CFSv2 with revised SAS as compared to old SAS scheme in simulating ISMR. It is clear (Fig. 3f) that the amount of precipitation over CI region has increased by 1 to 3 mm day^{-1} and over EIO it has decreased by 4 to 2 mm day^{-1} in revised SAS scheme compared to old SAS scheme. Overall, the revised SAS convective parameterization scheme in CFSv2 is able to reproduce the spatial distribution of mean state of the ISM rainfall better than the CFSv2 with old SAS scheme.

We find that the remarkable improvement of CFSv2 simulation of mean rainfall with revised SAS convection parameterization scheme over that of old SAS scheme lies in capturing the probability of occurrences of various rainfall categories. We evaluated the probability density distribution function (PDF) of rainfall over CI region (74°E–83°E, 18°N–26°N). Figure 4 shows the PDF of rainfall from TRMM (black curve), IMD (green curve), CFSv2 with revised SAS (blue curve) and CFSv2 with old SAS (red curve) over CI. The lighter rainfall (<10 mm day^{-1}) is found to have higher contribution to the observed total

rain from TRMM and IMD. Like many GCMs (Piani et al. 2010), CFSv2 with old SAS scheme shows serious problem in capturing the PDF of rain rate in general and the lighter rain rate in particular. It substantially overestimates the lighter rainfall and underestimates the moderate rain-rate (10–40 mm day^{-1}). Dai (2006) reported that the current GCMs have a tendency to overestimate the lighter rain. However, CFSv2 with revised SAS simulates the PDF of rain rate quite well as compared to observation. It is also of noticeable interest that even the PDF of lighter rain rate has been significantly improved.

In order to gain further insight on the simulated rainfall bias, we examine the area averaged smoothed annual cycle (AC) of rainfall over CI as exhibited in Fig. 5a. The smoothed climatology is computed from the first three harmonics of the daily climatology and annual mean. The AC of the monsoon is a reflection of the seasonal migration of the zonally oriented belt of precipitation or the intertropical convergence zone (ITCZ; Gadgil 2003). Figure 5a indicates that over CI, CFSv2 with old SAS scheme simulates a late onset and an early withdrawal thereby resulting a relatively shorter rainy season. The shorter length-of-the-rainy season is consistent
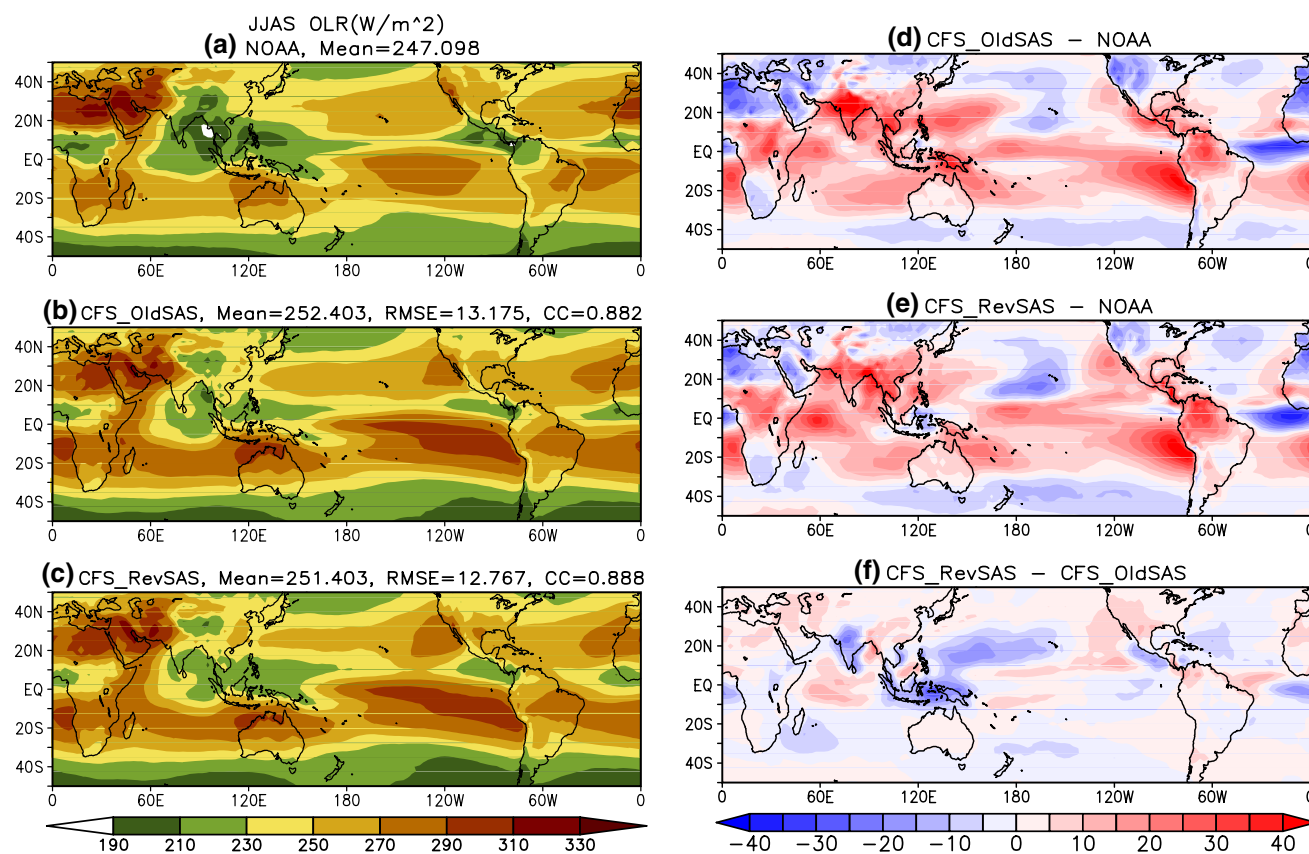
Fig. 2 JJAS mean climatological OLR (W m^{-2}) over global domain (50°N–50°S) from **a** NOAA, CFSv2 with **b** old SAS and **c** revised SAS scheme. Biases (W m^{-2}) in CFSv2 with **d** old SAS and **e** revised SAS scheme with respect to NOAA and **f** biases in CFSv2 with revised SAS with respect to old SAS scheme. Global mean OLR values are calculated for both observation and models (Fig. 2a–c). RMSE and pattern CC is calculated for old SAS (Fig. 2b) and revised SAS (Fig. 2c) with respect to NOAA

with the earlier findings by Sabeerali et al. (2012) and Goswami et al. (2014). This shorter rainy season bias is significantly improved in CFSv2 with revised SAS scheme where it is clearly visible that the onset of the monsoon is taking place almost simultaneously with the observation. The model is able to correctly reproduce the rapid enhancement in rainfall during the monsoon onset. However, the withdrawal appears to occur slightly earlier than observation and later than CFSv2 with old SAS scheme. The time-latitude section of rainfall averaged over core monsoon zone (70°E–90°E) is illustrated in Fig. 5b–d. In observation (TRMM) (Fig. 5d), the high rainfall band migrates up to 27°N causing considerable amount of precipitation over Indian land mass. On the other hand, CFSv2 with old SAS convection scheme (Fig. 5c) shows that most of the high rainfalls bands are mainly confined near the equator and very few of them are able to propagate up to 20°N. It eventually contributes to the huge rainfall dry bias over Indian land mass and wet bias over EIO. Similar problem of capturing northward migration of ITCZ rainfall in general circulation models is demonstrated by many earlier studies (Hack et al. 1998; Gates et al. 1999; Wu et al. 2003; Chaudhari et al.

2013). Figure 5b depicts the northward migration of ITCZ in CFSv2 with revised SAS scheme. It indicates that the high rainfall bands are able to migrate up to 20°N–25°N with considerable amount of rainfall over Indian land mass. CFSv2 with revised SAS scheme is able to capture more realistic northward migration of ITCZ precipitation than CFSv2 with old SAS scheme.

An investigation of the model's ability to simulate the eastward and northward propagation characteristics of summer monsoon intraseasonal variability (ISV) over ISM domain is shown in Fig. 6. The analysis is based on lag regressions of 10–90 day filtered precipitation with respect to a reference time series of 10–90 day filtered precipitation averaged over (70°E–90°E, 10°N–20°N). It is clearly visible that both models simulate the eastward (Fig. 6b, c) and northward (Fig. 6e, f) propagation reasonably well compared to TRMM observations (Fig. 6a, d). It is clear from the RMSE and pattern CC values that revised SAS is able to capture the northward and eastward propagation with better fidelity than old SAS scheme. Although CFSv2 with old SAS convection scheme is able to capture the
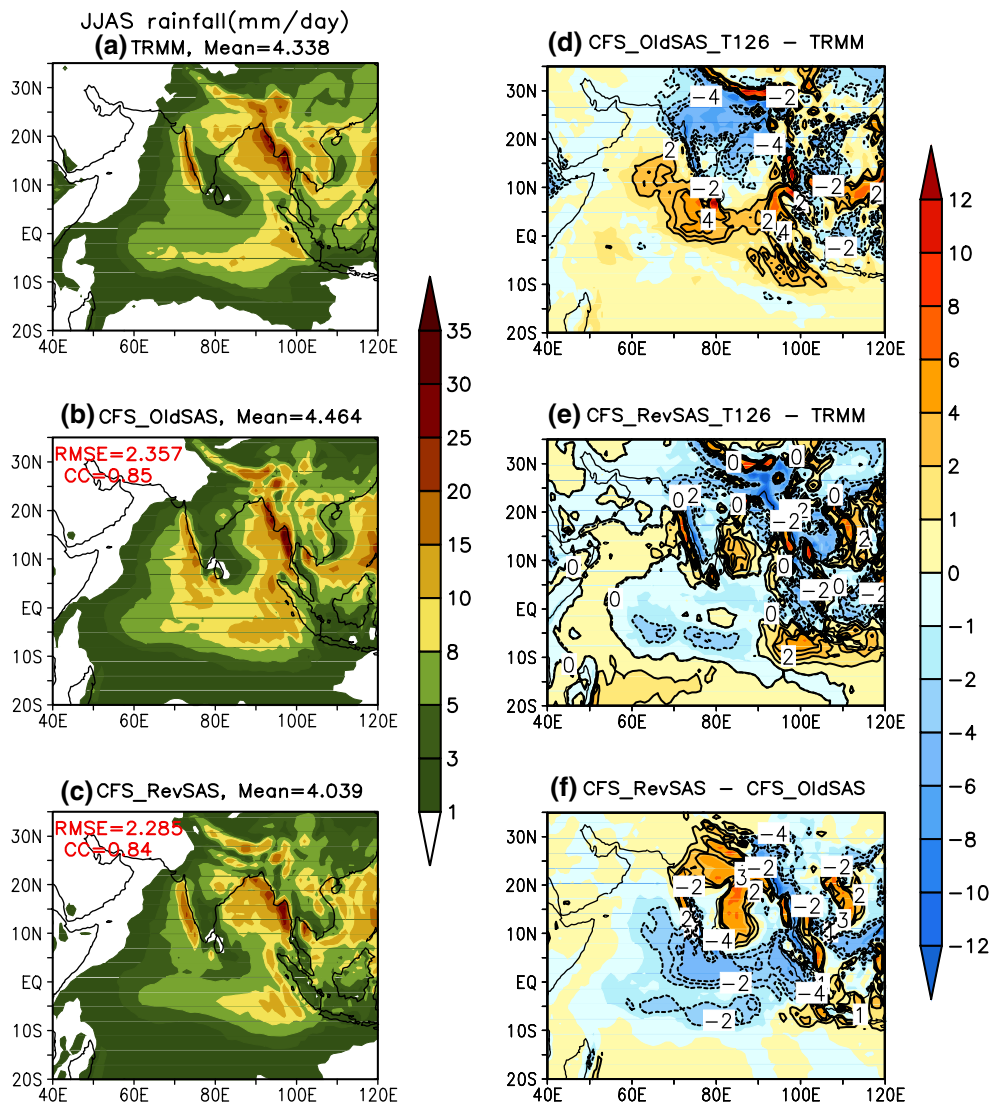
Fig. 3 JJAS mean climatological precipitation (mm day^{-1}) over Indian summer monsoon domain from **a** TRMM, CFSv2 with **b** old SAS and **c** revised SAS scheme. Biases (mm day^{-1}) in CFSv2 with **d** old SAS and **e** revised SAS scheme with respect to TRMM and **f** biases in CFSv2 with revised SAS with respect to old SAS scheme. Mean rainfall values are calculated for both observation and models (Fig. 3a–c). RMSE and pattern CC is calculated for old SAS (Fig. 3b) and revised SAS (Fig. 3c) with respect to TRMM

northward propagation, it has a huge dry bias over Indian land mass. Similar conclusions were reported by Saha et al. (2014), Sharmila et al. (2013) and Goswami et al. (2014) etc. On the other hand, CFSv2 with revised SAS scheme is capable of reproducing proper northward propagation as well as reasonable amount of rainfall over Indian land mass.

3.2 JJAS temperature and wind climatology

The climatological mean temperature profile is not captured reasonably in CFSv2 with old SAS and revised SAS simulations compared to NCEP as indicated in Fig. 7. To check whether temperature bias in CFSv2

exists throughout the troposphere or at any particular level, we have analyzed the vertical profile of JJAS mean temperature averaged over global tropics (Fig. 7a) and over ISM domain (Fig. 7b) respectively. The analyses reveal that over tropics, both SAS schemes in CFSv2 show almost similar pattern (Fig. 7a, red and blue line) and underestimate the mean temperature throughout the troposphere as compared to NCEP (Fig. 7a, black line). The similar scenario can be seen over ISM domain (Fig. 7b) where both SAS schemes underestimate the air temperature all over the troposphere. The atmosphere of CFSv2 with both SAS schemes appears colder than observation (Fig. 7) which is consistent with earlier studies (Saha et al. 2014) with old SAS scheme.
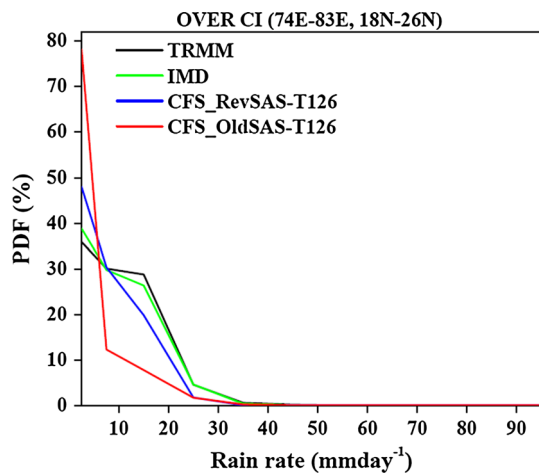
Fig. 4 Percentage of PDF of rainfall rate based on JJAS daily data over CI from TRMM (*black line*), IMD (*green line*), CFSv2 with old SAS (*red line*) and revised SAS (*blue line*) scheme

The ISM is characterized by a strong low level south westerly jet known as Findlater Jet (Findlater 1969), which peaks at around Somali coast and Arabian sea region. The 850 hPa JJAS mean circulation is displayed in Fig. 8a–c. A noticeable feature of the CFSv2 with revised SAS simulation is the dominant presence of the zonal component of the monsoon cross equatorial low level jet (LLJ) (Fig. 8c). CFSv2 with both SAS schemes mimic the observation somewhat realistically but the strength of the LLJ is quite weak in old SAS as compared to that of NCEP (Fig. 8a–c). Similar results were reported by Chaudhari et al. (2013) by analyzing 30 years of CFSv1 free run with old SAS scheme. Careful observation reveals that the LLJ in CFSv2 with revised SAS scheme is much stronger (Fig. 8e) than old SAS simulation. Another noteworthy feature of the CFSv2 with revised SAS simulation is that the strength of the LLJ over BoB is intensified (Fig. 8c, e) as compared to CFSv2 with old SAS simulation (Fig. 8f) and it agrees with the observation (Fig. 8a) particularly over the
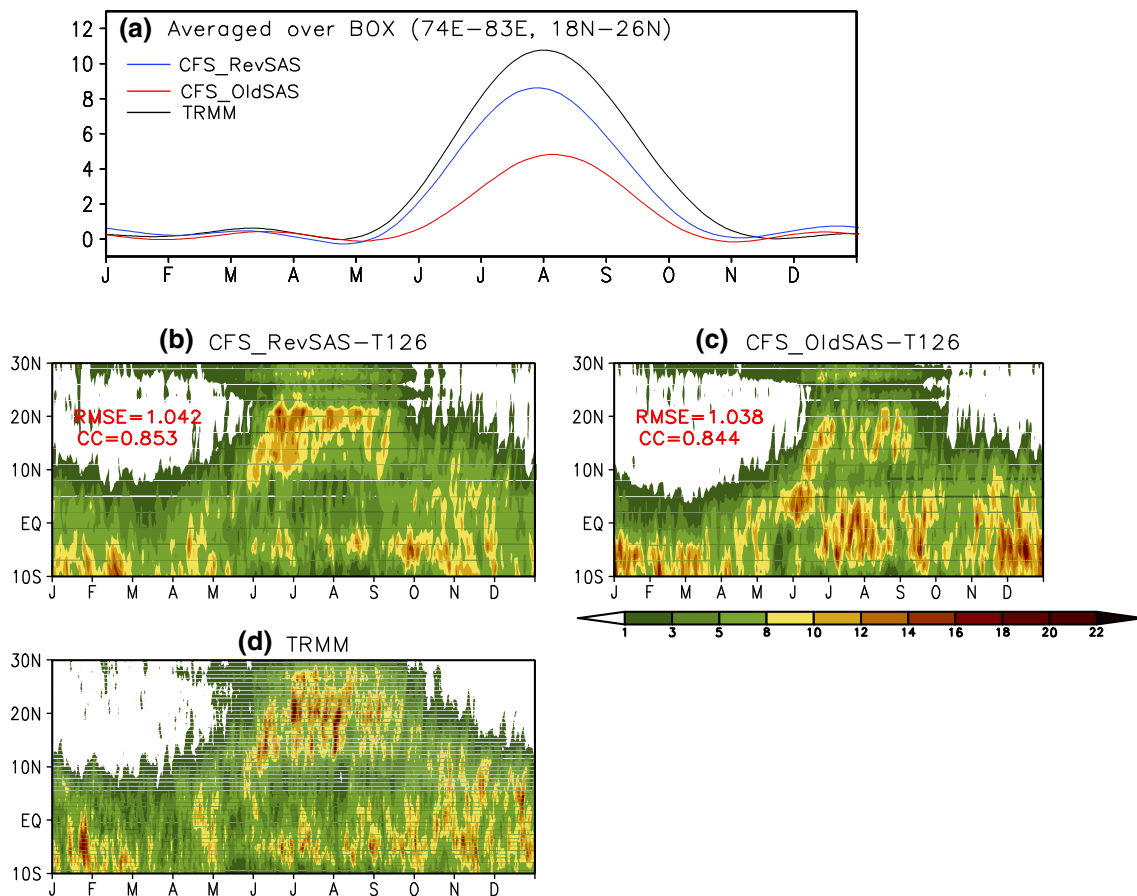

Fig. 5 a The area averaged smoothed (first 3 harmonics plus mean) annual cycle of climatological rainfall (mm day^{-1}) averaged over CI from TRMM (*black line*), CFSv2 with old SAS (*red line*) and revised SAS (*blue line*) scheme. Time-latitude section of rainfall (mm day^{-1}) from **b** CFS2 with revised SAS, **c** CFSv2 with old SAS scheme and **d** TRMM averaged over 70°E–90°E. RMSE and pattern CC is calculated for revised SAS (Fig. 5b) and old SAS (Fig. 5c) with respect to TRMM
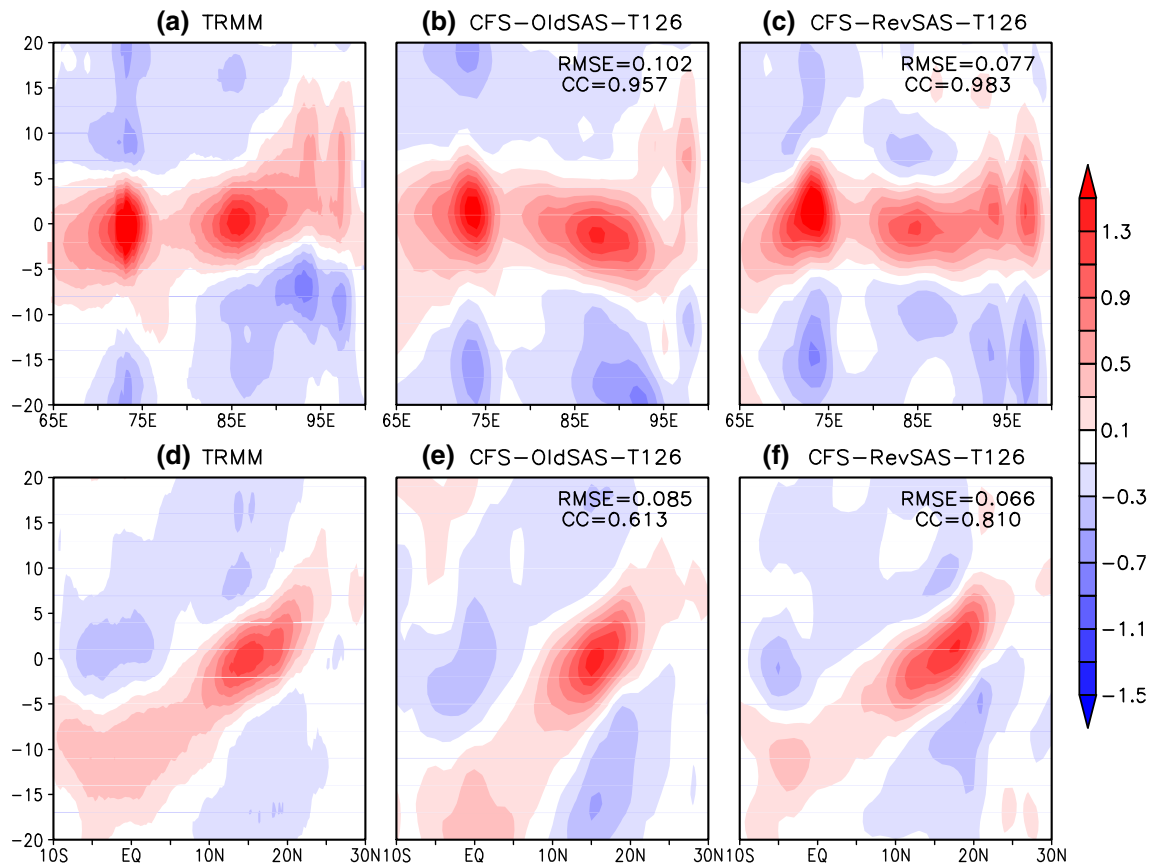
Fig. 6 **a** Longitude-time and **d** latitude-time plots of 10–90 day filtered TRMM precipitation anomalies regressed on a reference time series, averaged over 10°N–20°N and 70°E–90°E, respectively. **b**, **e** and **c**, **f** Same as Fig. 5a, d but for CFSv2 with old SAS and revised SAS scheme, respectively. RMSE and pattern CC is calculated for old SAS (Fig. 6b, e) and revised SAS (Fig. 6c, f) with respect to TRMM
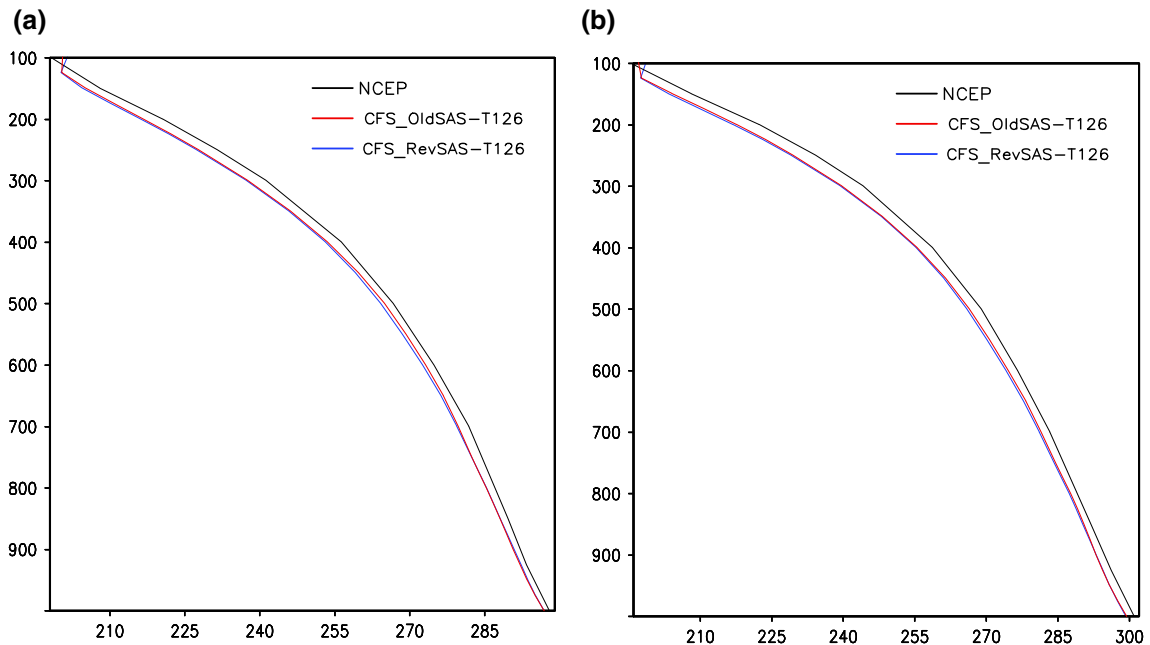

Fig. 7 Vertical temperature profile during JJAS averaged over **a** global tropics (30°S–30°N) and **b** ISM domain (60°E–100°E, 10°S–30°N)
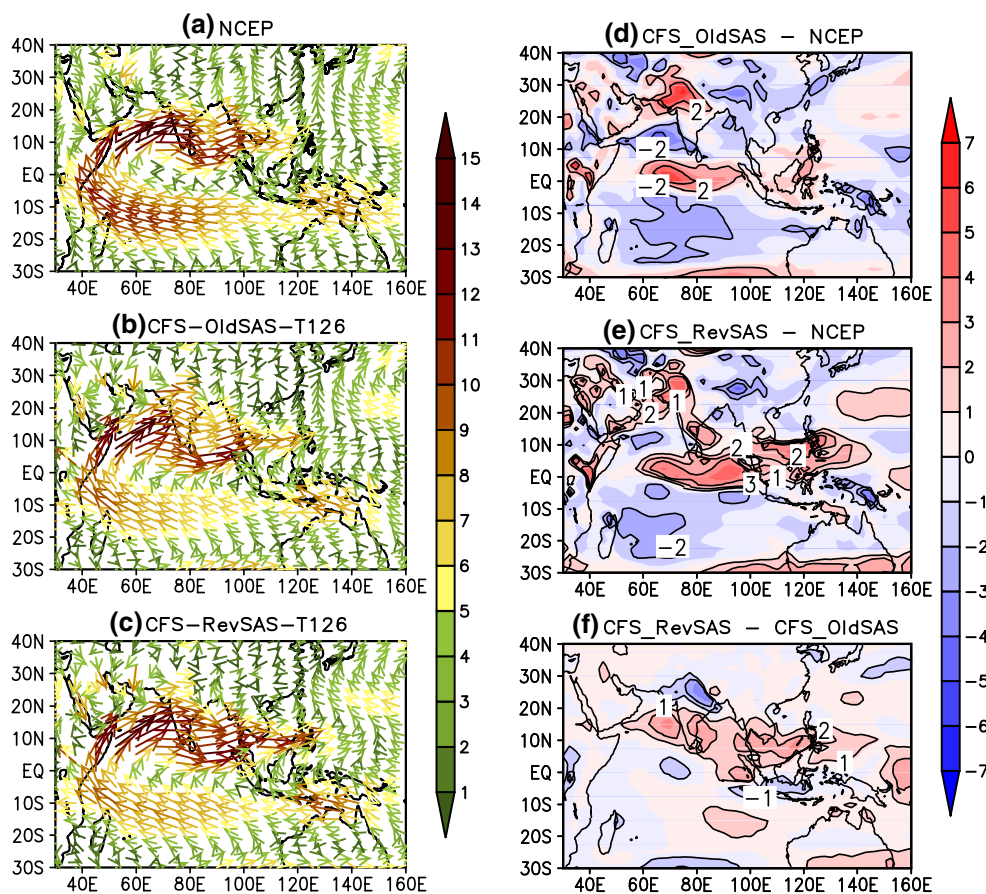
Fig. 8 JJAS mean climatological 850 hPa winds (ms^{-1}) for **a** NCEP, CFSv2 with **b** old SAS and **c** revised SAS scheme. Biases (ms^{-1}) in CFSv2 with **d** old SAS and **e** revised SAS scheme with respect to NCEP and **f** biases in CFSv2 with revised SAS with respect to old SAS scheme

central BoB. The characteristic feature of the upper tropospheric circulation at 200 hPa is the tropical easterly jet (TEJ) over the southern India and adjoining EIO (Fig. 9a). Strength of the TEJ provides an indication of monsoon activity over the Indian subcontinent (Naidu et al. 2011). CFSv2 with both SAS schemes are able to simulate TEJ over the southern India and adjoining Indian Ocean (Fig. 9b, c). However, the strength of the TEJ is found to be higher in revised SAS simulation as compared to old SAS simulation (Fig. 9d–f). Enhanced strength of the upper tropospheric easterlies in the simulation of CFSv2 with revised SAS has helped to improve the negative bias of easterlies simulated by old SAS (Fig. 9d, e).The position of the Tibetan High is also reasonably simulated by CFSv2 with both SAS schemes compared to observations (Fig. 9a–c).

3.3 Tropospheric temperature

Tropospheric temperature (TT) is defined as the air temperature averaged between 600 and 200 hPa following

Xavier et al. (2007). The north–south gradient of TT over Indian subcontinent region is essential in order to sustain the monsoon circulation (Webster et al. 1998; Goswami and Xavier 2005) and it is also closely linked with the onset and withdrawal of ISM (Ueda and Yasunari 1998; Goswami and Xavier 2005; Xavier et al. 2007). The JJAS mean TT is shown in Fig. 10a–c. Mean seasonal TT is characterized by elevated heat source of Tibetan plateau and high TT throughout the tropics as seen in NCEP reanalysis (Fig. 10a). CFSv2 with both SAS schemes are able to reproduce the warm troposphere over Tibetan plateau (Fig. 10b, c). However, CFSv2 with both SAS schemes underestimate the mean TT throughout the tropics (Fig. 10d, e). Saha et al. (2014) reported similar cold TT bias in CFSv2 with old SAS scheme. Relative improvement in CFSv2 with revised SAS scheme can be seen over northern part of Indian subcontinent and eastern tropical pacific region (Fig. 10f) compared to CFSv2 with old SAS scheme. Thus, the TT does not look very reasonable in CFSv2 (as seen by global mean and RMSE) with revised SAS as compared to NCEP.
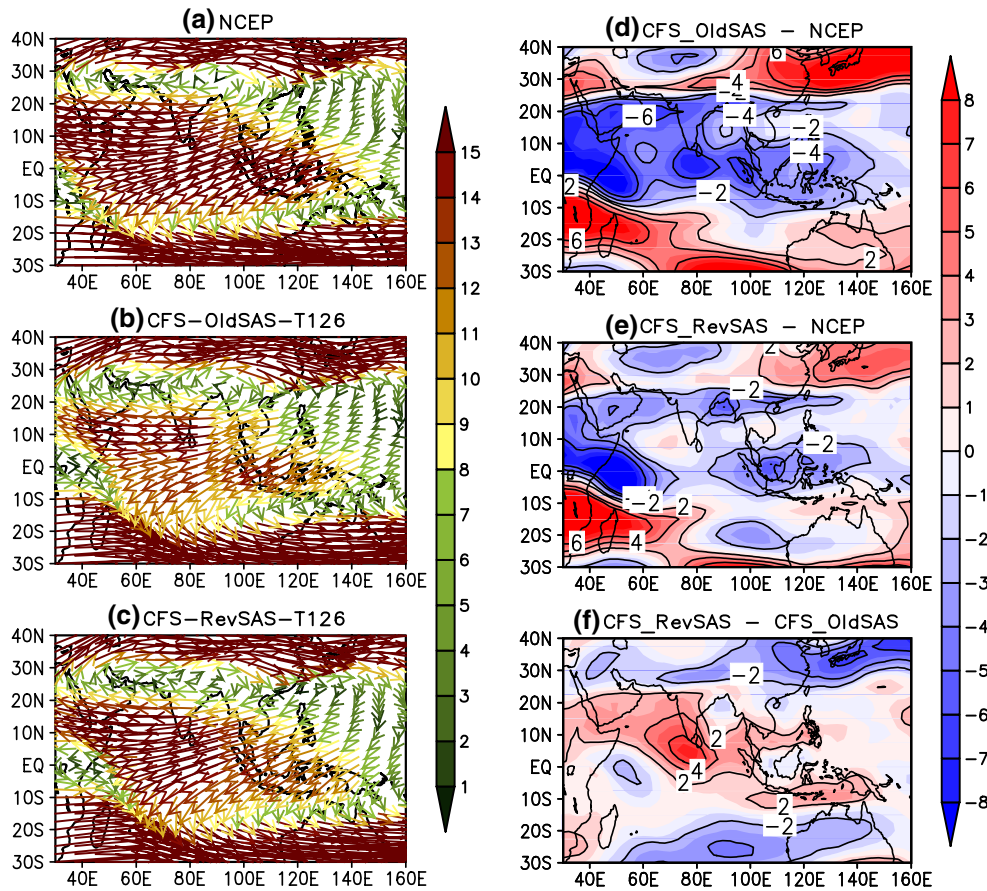
Fig. 9 JJAS mean climatological 200 hPa winds (ms^{-1}) for **a** NCEP, CFSv2 with **b** old SAS and **c** revised SAS scheme. Biases (ms^{-1}) in CFSv2 with **d** old SAS and **e** revised SAS scheme with respect to NCEP and **f** biases in CFSv2 with revised SAS with respect to old SAS scheme

3.4 Convective rainfall

In the present study, we have changed old SAS scheme to revised SAS deep convective parameterization scheme in CFSv2 following Han and Pan (2011). Thus, it will be interesting to see the impact of revised SAS scheme in simulating convective rainfall during JJAS. Convective rainfall causes maximum heating at the middle level of the troposphere and affects the associated atmospheric dynamics (Houze 1989). The JJAS mean convective rainfall is shown in Fig. 11a–c. Mean convective rainfall is considerably underestimated over Indian landmass by CFSv2 with old SAS scheme (Fig. 11b) as compared to observation (Fig. 11a). However, CFSv2 with revised SAS scheme shows noticeable enhancement of convective rainfall over Indian landmass region (Fig. 11c). CFSv2 with both SAS schemes overestimate the convective rainfall over equatorial Pacific Ocean, EIO and west coast of Africa region (Fig. 11b, c) as compared with the observation (Fig. 11a).

It is likely that the improvement of convective rainfall over Indian landmass during monsoon season is due to the proper simulation of the probability of occurrences of various convective rainfall categories. Figure 12 shows the PDF of convective rainfall from TRMM 3G68 (black line), CFSv2 with old SAS (red line) and with revised SAS scheme (blue line) over CI. The lighter category (<10 mm day^{-1}) of convective rainfall is found to have higher contribution to total convective rainfall for both observation and models. However, CFSv2 with old SAS scheme overestimates the lighter convective rainfall and underestimates the moderate category (Fig. 12). On the other hand, this bias is substantially improved in CFSv2 with revised SAS simulation which agrees well with the observation.

Apart from convective rainfall, stratiform rainfall also plays a significant role in modulating the monsoon ISOs (Chattopadhyay et al. 2009). However, in the present study, we have seen (Fig. not shown) that stratiform rainfall distribution and its PDF has not improved in revised SAS simulation. Therefore, it appears that the total rainfall PDF
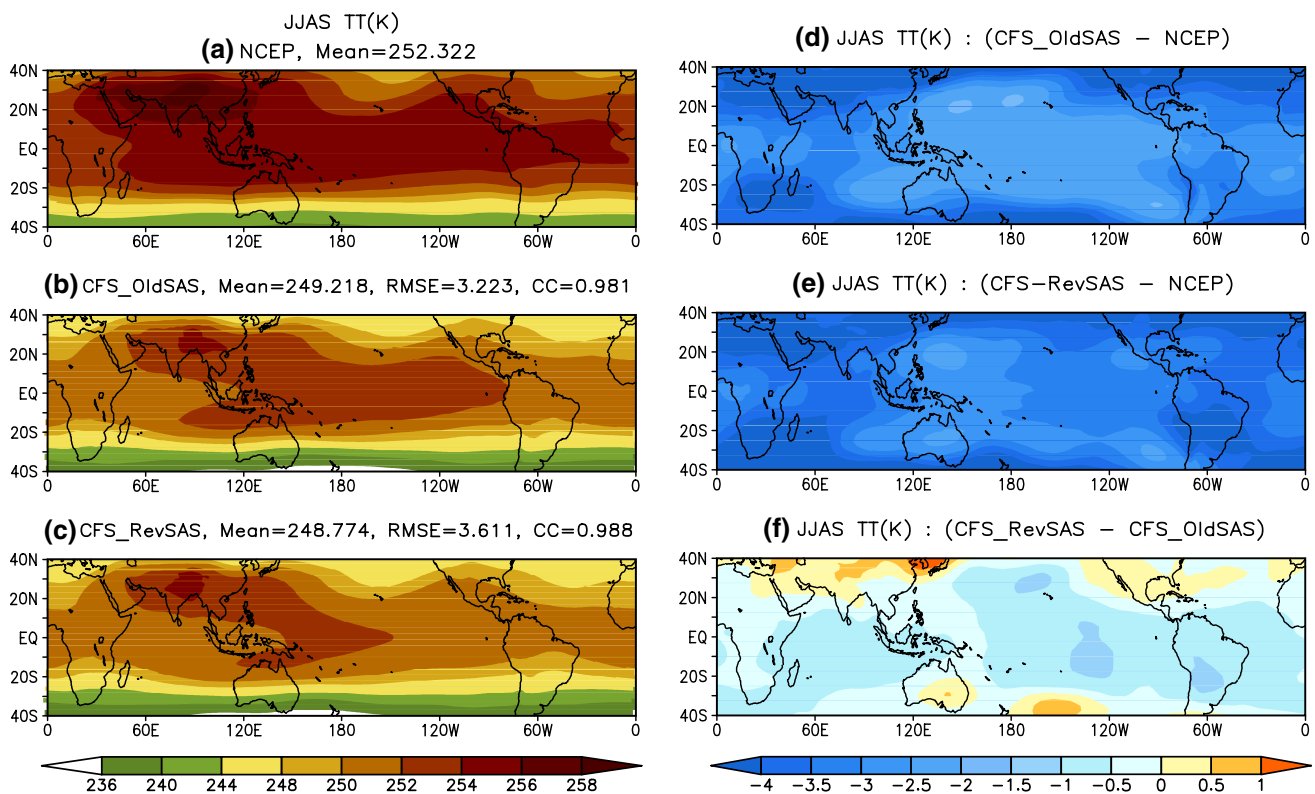
Fig. 10 JJAS mean climatological tropospheric temperature (K) from **a** NCEP, CFSv2 with **b** old SAS and **c** revised SAS scheme. Biases (K) in CFSv2 with **d** old SAS and **e** revised SAS scheme with respect to NCEP and **f** biases in CFSv2 with revised SAS with respect to old SAS scheme. Global mean TT values are calculated for both observation and models (Fig. 10a–c). RMSE and pattern CC is calculated for old SAS (Fig. 10b) and revised SAS (Fig. 10c) with respect to NCEP

improvement in CFSv2 with revised SAS (Fig. 4) scheme is mainly contributed by better simulation of convective rainfall PDF.

3.5 Evaluation of low and high clouds

Earth's climate system is largely modulated by clouds which play a crucial role in regulating Earth's energy budget and water cycle (Rossow and Zhang 1995; Barker et al. 1999; Collins 2001). Thus, it will be important to analyze the impact of revised SAS in simulating cloud features during JJAS. Figure 13a–c shows the global distributions of low level cloud fractions estimated from ISCCP data and CFSv2 model simulations. The observation from ISCCP shows extensive marine stratocumulus clouds over the eastern tropical Pacific and Atlantic oceans (Fig. 13a), such distributions of low clouds are not well-simulated by CFSv2 with both SAS schemes (Fig. 13b, c). Models appear to underestimate low clouds over these regions. Recently, Yoo et al. (2013) showed underestimation of low clouds over tropical Pacific and Atlantic oceans in NCEP Global Forecast System (GFS) model. However, in the present study, the low clouds

appear to be overestimated in both SAS schemes as compared to ISCCP over Indian landmass (Fig. 13b, c). On the other hand, the spatial distributions of high cloud fractions throughout the globe are captured by CFSv2 with both SAS schemes (Fig. 13d–f). Both models overestimate the high cloud fractions over tropical Pacific Ocean, west coast of Africa and EIO (Fig. 13e, f). It is interesting to note that the high clouds particularly over Indian landmass are enhanced in revised SAS simulation which agrees with the observation (Fig. 13d, f). From the global (60°S–60°N) mean values, it appears that both models simulate less low clouds and more high clouds.

3.6 Simulation of diurnal scale precipitation, OLR, clouds and apparent heat source (Q1) over central India

The above analyses documented the impact of revised SAS in CFSv2 in simulating various parameters. The daily scale analysis of rainfall during JJAS showed significant improvement in spatial distribution over ISM domain (Fig. 3). However, it will be important to analyze whether the daily scale rainfall improvement is actually coming from the sub-daily
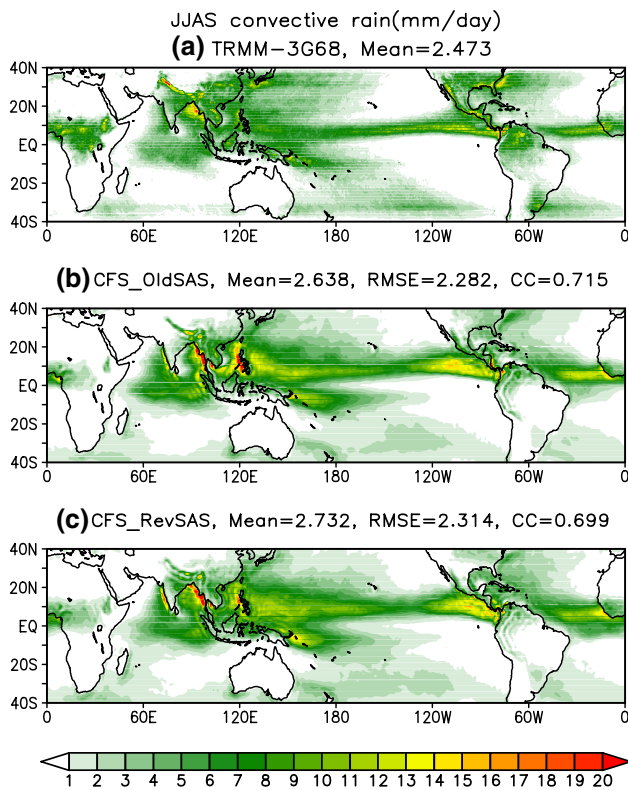
Fig. 11 JJAS mean climatological convective rainfall (mm day^{-1}) from **a** TRMM 3G68, CFSv2 with **b** old SAS and **c** revised SAS scheme. Global mean convective rainfall values are calculated for both observation and models (Fig. 11a–c). RMSE and pattern CC is calculated for old SAS (Fig. 11b) and revised SAS (Fig. 11c) with respect to TRMM 3G68
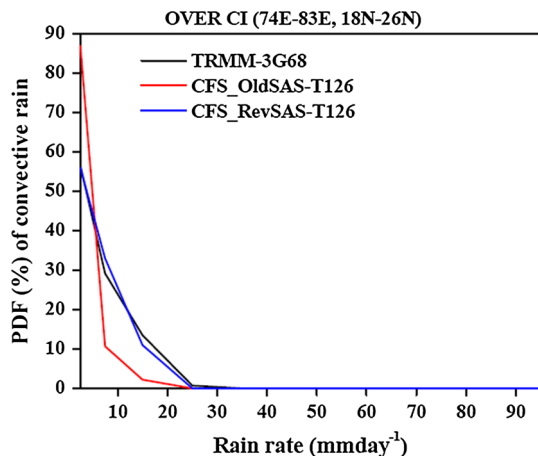

Fig. 12 Percentage of PDF of convective rainfall rate based on JJAS daily data over CI for TRMM 3G68 (*black line*), CFSv2 with old SAS (*red line*) and revised SAS (*blue line*) scheme

scale? To identify that, firstly, we have analyzed the diurnal cycle of OLR and rainfall over CI as indicated in Fig. 14a, b, respectively. The diurnal cycle of OLR shows a clear

maximum at 1130 Indian Standard Time (IST) in observation (dot-dash black line in Fig. 14a) whereas the CFSv2 with old SAS scheme at T126 and T382 resolution is unable to capture the magnitude as well as the time of maximum of the diurnal cycle. It appears that CFSv2 with old SAS scheme at both the resolutions overestimate the OLR and reaches maximum at around 1430 IST. On the other hand, CFSv2 with revised SAS scheme shows (Fig. 14a, blue line) similar diurnal cycle of OLR as old SAS scheme; however, the magnitude of OLR is reduced and agrees with Kalpana-1.

The diurnal cycle of precipitation over CI shows a clear maximum at 1730 IST (Fig. 14b, dash black line) in observation consistent with typical continental regime characterized by an afternoon-late evening peak (Yang and Smith 2006). CFSv2 with old SAS scheme simulation does not reproduce proper diurnal cycle of precipitation and maximizes at 1430 IST for both resolutions (T126 and T382). This implies that the diurnal cycle of convection possibly is not captured realistically by the model. Several studies (Betts and Jakob 2002; Dai and Trenberth 2004; Lee et al. 2007; Dirmeyer et al. 2010) have pointed out that the global general circulation models have a tendency to simulate observed late-afternoon rainfall peak too early in the day and this premature peak in convection is a well-known problem with many cumulus parameterization schemes. However, the revised SAS scheme in CFSv2 is found to capture the timing of maximum precipitation at around 1730 IST similar to what is seen in TRMM (Fig. 14b); although it overestimates the magnitude.

Further we would like to examine the improvement in diurnal cycle of rainfall in revised SAS and associated rainfall PDF over CI. TRMM estimated rainfall PDF (Fig. 15a) shows that the occurrence of lighter rain rates (0.0–0.5 mm h^{-1}) are relatively more during early morning (0230 IST) to late morning (1130 IST) hours, whereas, moderate rainfall (0.5–2.0 mm h^{-1}) dominates during the early afternoon (1430 IST) to late evening (2030 IST) hours. CFSv2 with old SAS scheme at T126 and T382 resolution simulates nearly similar PDF for all the time throughout the day (Fig. 15b, d). It appears that the old SAS scheme is unable to capture the PDF of lighter and moderate category rainfall at different times over CI. The revised SAS in CFSV2 shows significant improvement in simulating diurnal rainfall PDF over CI (Fig. 15c). The revised SAS is able to separate out lighter and moderate category rainfall at different times similar to TRMM analysis. However, it overestimates moderate and heavier category rainfall possibly due to the way the new instability removal is applied in revised SAS.

The rainfall PDF analyses gave us an idea about which rainfall category is dominant at what times during the day over CI. At the same time, it will be useful to know the amount of rainfall contributed by each hour to the daily total rainfall. Figure 16 demonstrates the percentage of
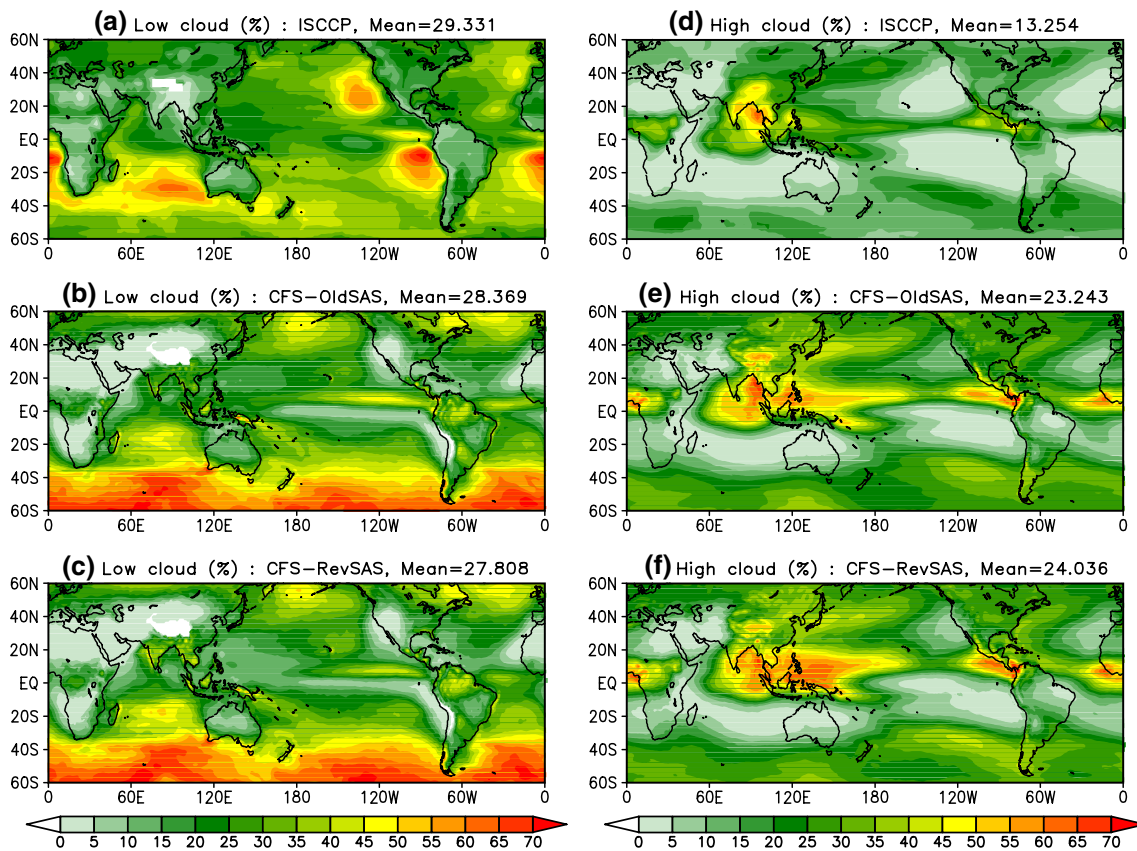
Fig. 13 JJAS mean climatological low cloud fractions (%) for **a** ISCCP, CFSv2 with **b** old SAS and **c** revised SAS scheme. **d**–**f** Same as Fig. 11a–c but for high cloud fractions. Global mean cloud fractions are calculated for both observation and models (Fig. 13a–f)

Fig. 14 JJAS climatology of **a** OLR (W m^{-2}) and **b** rainfall (mm h^{-1}) over CI. For each panel, *red line* is for CFSv2-OldSAS-T126, *green line* for CFSv2-OldSAS-T382 and *blue line* is for CFSv2-revised SAS-T126. The *black line* in **a** is for Kalpana-1and for **b** TRMM
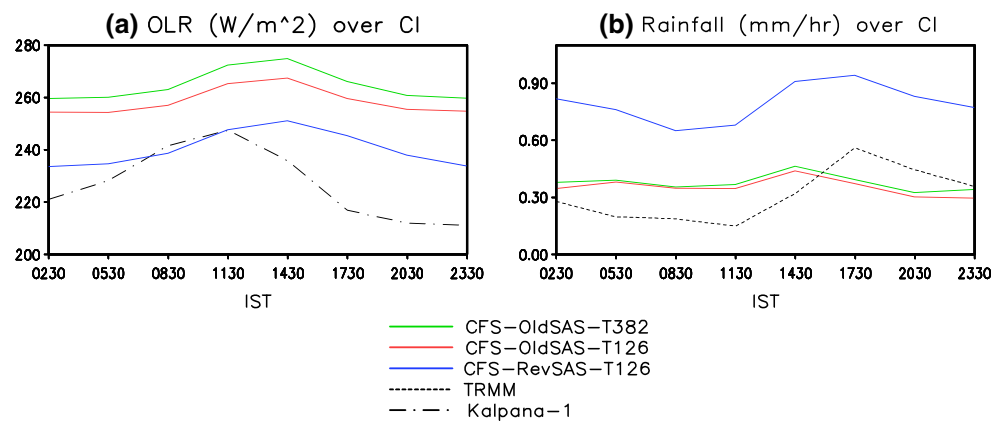
rainfall contribution by each hour to the daily total rainfall during JJAS over CI. TRMM estimation shows that maximum contribution to daily rain occurs at 1730 IST, whereas, CFSv2 with old SAS scheme completely fails to reproduce the observed features and shows maximum contribution during early morning hours for both resolutions. On the other hand, CFSv2 with revised SAS scheme is able to capture the diurnal cycle of contribution to daily total and maximum contribution is seen during afternoon

hour (1730 IST). However, it underestimates the percentage of maximum contribution to daily total as compared to observation.

To get more insight about type of cloud responsible for observed or simulated diurnal cycle of rainfall over CI, we have analyzed the diurnal cycle of low clouds and high clouds fractions during JJAS as shown in Fig. 17a, b, respectively. ISCCP estimated low clouds maximizes at around 1130–1430 IST (Fig. 17a, black line), whereas CFSv2 with
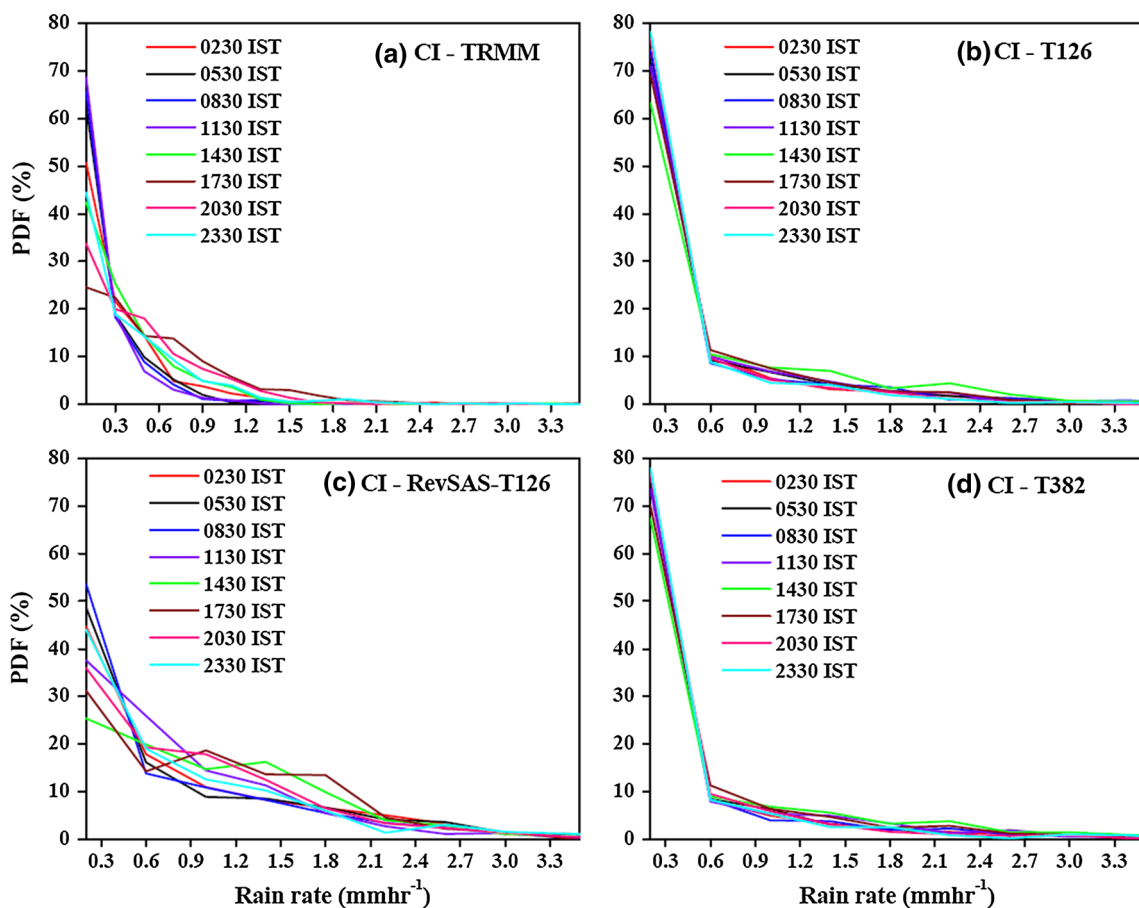
Fig. 15 Percentage of PDF of rainfall rate over CI from **a** TRMM, CFSv2 with **b** old SAS at T126 resolution, **c** revised SAS at T126 resolution and **d** old SAS at T382 resolution corresponding to the eight octets,0230 IST through 2330 IST at 3-hourly intervals
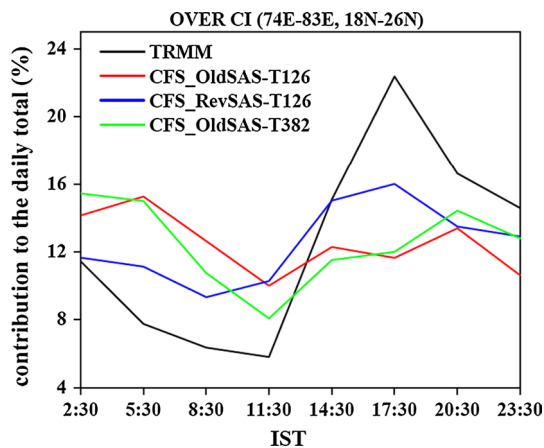

Fig. 16 Percentage of contribution to the daily total rainfall by eight octets,0230 IST through 2330 IST at 3-hourly intervals over CI for TRMM (*black line*), CFSv2 with old SAS (*red line*) at T126 resolution, revised SAS (*blue line*) at T126 resolution and old SAS at T382 resolution (*green line*)

old SAS (T126) and revised SAS schemes peak at around 1730 IST and they overestimate low clouds fractions as compared to ISCCP. CFSv2 with old SAS scheme at T382 resolution also simulates peak low clouds fraction at 1730 IST, however, it is able to capture the magnitude similar to observation. The high clouds fractions appear to be maximized in the afternoon to late afternoon hours in observation (Fig. 17b, black line). It is likely that the observed afternoon rainfall maximum over CI could be due to the presence of deep convection and associated high clouds during that time (Qie et al. 2014). CFSv2 with old SAS scheme at both resolutions show very weak diurnal cycle of high clouds and substantially underestimate the high clouds fractions (Fig. 17b). On the other hand, the revised SAS in CFSv2 is able to realistically simulate the diurnal cycle of high clouds fractions although the amplitude is underestimated.

After evaluating rainfall biases and demonstrating the improvement of rainfall distribution by revised SAS, it will be
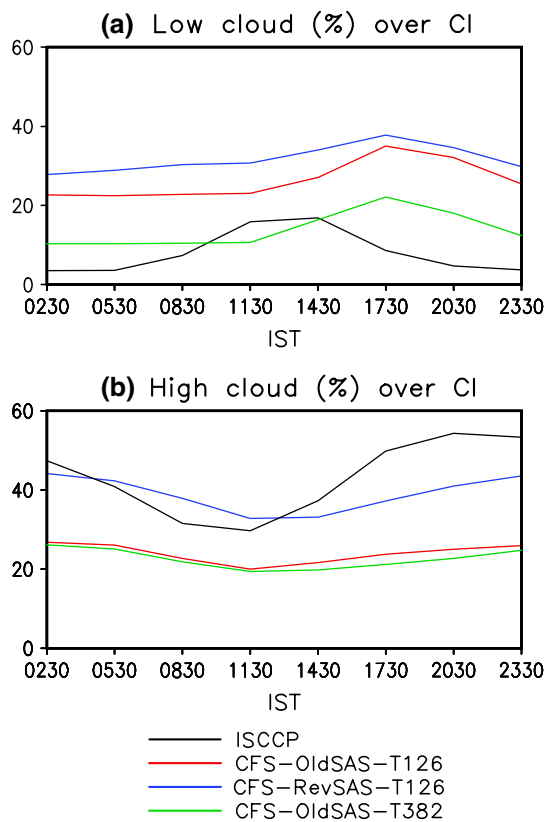
Fig. 17 JJAS climatology of **a** low cloud fractions (%) and **b** high cloud fractions (%) over CI. For each panel, *red line* is for CFSv2-OldSAS-T126, *green line* for CFSv2-OldSAS-T382 and *blue line* is for CFSv2-revised SAS-T126. The *black line* in **a** and **b** is for ISCCP

Fig. 18 JJAS domain-averaged (40°E–140°E, 10°N–35°N) apparent heat source Q1 (K day^{-1}) for CFSv2 with old SAS (*red*) and revised SAS (*blue*) scheme

worthwhile to evaluate the heating of the revised SAS as compared to old SAS. As, heating will reflect the strength of the convection. In view of this, apparent heat source (Q1) is computed based on Yanai et al. (1973). The Q1 profile (Fig. 18) averaged over (40°E–140°E, 10°N–35°N), shows that the revised SAS has produced a stronger heating compared to default SAS indicating enhanced convection in revised SAS.

The above analyses indicate that improvement of convective parameterization (revised SAS in this case) could make a significant impact in improving the rainfall bias of ISM which could not be achieved by increasing the horizontal resolution alone. However, it is noticed that all the systematic biases (e.g. tropospheric temperature, low cloud etc.) have not improved in revised SAS simulation which actually leaves us lots of scope for future model development.

3.7 Impact of shallow convection scheme in revised SAS of CFSv2

The previous analyses have shown the impact of revised SAS deep convective parameterization scheme in CFSv2
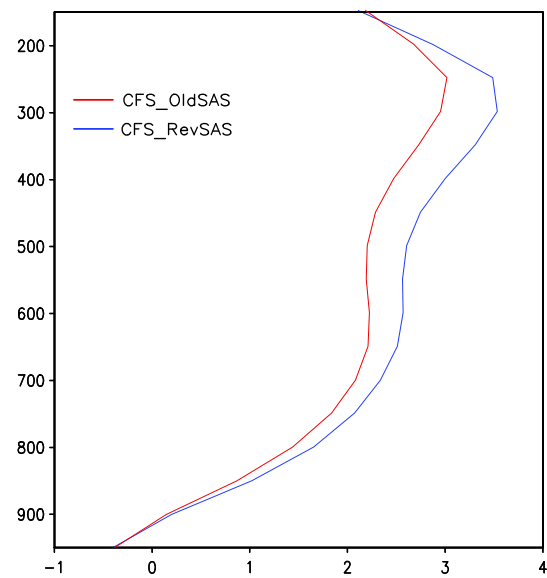
in simulating ISM features. The modification in SAS deep convective scheme has been done based on the study by Han and Pan (2011). However, their study also includes the application of revised version of shallow convection (SC) scheme which we did not use in the above analyses. The major difference between the old and new SC schemes is implementation of a mass flux parameterization replacing the old turbulent diffusion-based approach (Han and Pan 2011). It will be interesting to see how both the revised versions of SC and deep convection schemes in CFSv2 are able to reproduce some of the observed ISM features. In addition to revised SC and deep convection schemes, we have also modified the critical vertical velocities following Lim et al. (2014). In the old SAS and revised deep SAS scheme, the critical vertical velocity thresholds are kept constant throughout the globe, whereas in the modified version, the critical vertical velocity thresholds are made (w2 = −250/dx, w1 = 0.1*w2, dx-grid size in meter) grid size dependent. After incorporating all these modification, we have made 8 years of CFSv2 free run with the same initial condition as earlier free runs.

Figure 19a–c indicates the global rainfall distribution during JJAS. It is clear that the rainfall overestimation over northern equatorial west Pacific region is reduced in revised SC scheme compared to old SAS scheme and it reasonably agrees with the observation (Fig. 19a–c). In fact, it is able to simulate better rainfall distribution over northern part of west Pacific and African landmass region compared to revised SAS deep convection scheme (Fig. 1c). However, the revised SC scheme underestimates the rainfall amount
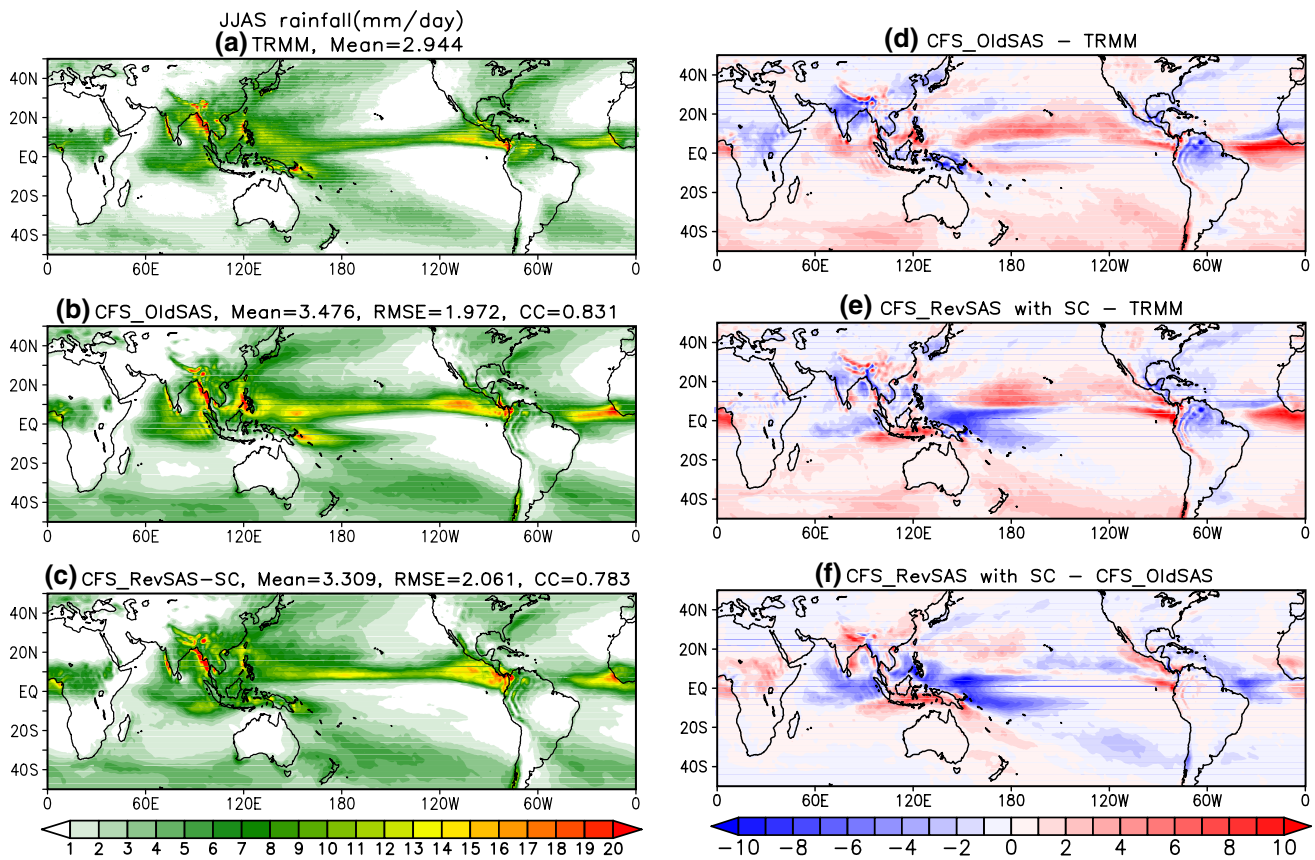
Fig. 19 JJAS mean climatological precipitation (mm day^{-1}) over global domain (50°N–50°S) from **a** TRMM, CFSv2 with **b** old SAS and **c** revised SAS having SC scheme. Biases (mm day^{-1}) in CFSv2 with **d** old SAS and **e** revised SAS having SC scheme with respect to TRMM and **f** biases in CFSv2 with revised SAS having SC with respect to old SAS scheme. Global mean rainfall values are calculated for both observation and models (Fig. 18a–c). RMSE and pattern CC is calculated for old SAS (Fig. 18b) and revised SAS (Fig. 18c) with respect to TRMM

over southern equatorial Pacific region (Fig. 19e). Over Indian landmass, it simulates more rainfall than old SAS scheme (Fig. 19f), however, the amount of rainfall is less than the revised SAS deep convection scheme simulation (Fig. 1c). Similar overestimation of rainfall over east Pacific and west coast of Africa can be seen in revised SC scheme as compared to old SAS scheme (Fig. 19b, c). Convective rainfall distribution is also improved over west pacific and African landmass in revised SC scheme simulation (Fig. 20c) compared to old SAS (Fig. 20b) and revised deep convection schemes (Fig. 11c). The enhancement of convective rainfall over Indian landmass can be seen in Fig. 20c; however, it is less than the revised SAS deep convection scheme simulation (Fig. 11c). The revised SC scheme is also found to overestimate convective rainfall over east pacific and west coast of Africa region (Fig. 20c) as old SAS and revised deep convection scheme (Fig. 11b, c). Thus, the implementation of SC in revised SAS has not been able to make more improvement than that by revised SAS with deep convective scheme. To quantify the

improvements, we have compared the tropospheric temperature and it is found to be even cooler than that of the revised SAS with deep convection run (figures not shown). This indicates that revised SAS with the deep convection scheme appears to produce more realistic results for ISM simulation. To improve the large scale precipitation, a possible improvement in the model cloud microphysics is needed.

4 Summary and conclusions

In the present study, we intend to examine the ability of the revised SAS deep convection parameterization scheme in CFSv2 model to simulate the spatio-temporal variability of the mean ISM. The implementation of revised SAS scheme is based on the study by Han and Pan (2011). We have made two free runs experiments each for 15 years of CFSv2-T126, one with default/old SAS convection scheme and another with revised SAS scheme with the same initial
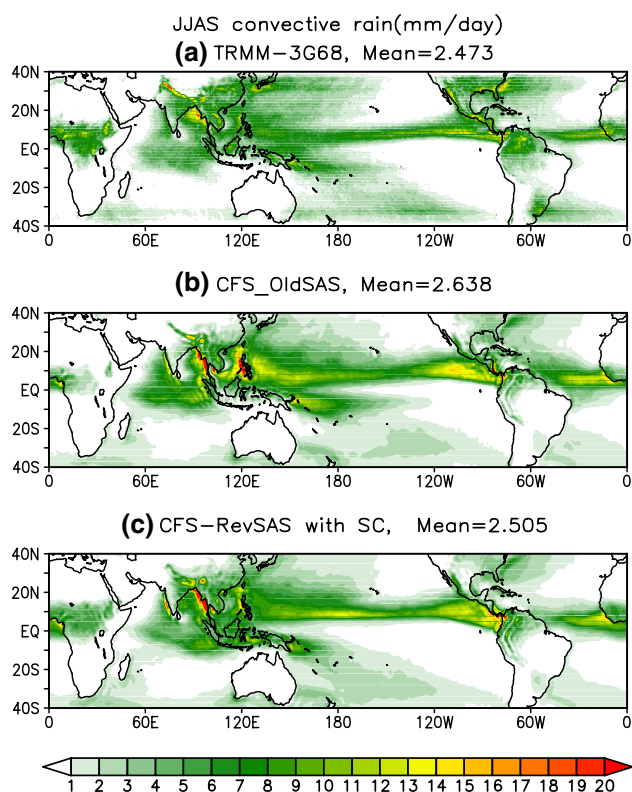
Fig. 20 JJAS mean climatological convective rainfall (mm day^{-1}) from **a** TRMM 3G68, CFSv2 with **b** old SAS and **c** revised SAS having SC scheme. Global mean convective rainfall values are calculated for both observation and models (Fig. 19a–c)

condition. Both these experiments are carried out with daily output. The diagnosis reveals that the positive precipitation bias over the equatorial Pacific and west coast of Africa in CFSv2 with old SAS simulations has reduced in revised SAS. The OLR distributions over Indian land mass and western Pacific Ocean have been improved in revised SAS simulation. The most significant improvement has been seen in simulating ISM precipitation. The long-standing inability to reduce the dry bias over Indian land-mass and wet bias over equatorial Indian Ocean in many GCMs appears to be largely resolved in revised SAS simulation. Overall, CFSv2 with revised SAS simulation is able to reproduce better spatial distribution of rainfall over ISM domain. It is found that model's better fidelity in simulating mean precipitation over Indian landmass with revised SAS scheme, lies in capturing proper rainfall PDF. CFSv2 with revised SAS scheme is able to simulate the PDF of rain rate quite well as compared to observation over CI. Particularly, lighter rain rate category is found to significantly improve in revised SAS simulation. However, CFSv2 with old SAS scheme highly overestimates lighter rainfall category, while moderate rain event are less frequent than the observation, resulting dry bias over Indian landmass. The area averaged

smoothed (first 3 harmonics plus mean) annual cycle of rainfall over CI is better captured in revised SAS scheme. It is found that CFSv2 with old SAS scheme simulates a late onset and an early withdrawal thereby resulting a relatively shorter rainy season. However, shorter rainy season bias is much improved in CFSv2 with revised SAS scheme as compared to observation. The northward migration of ITCZ is reasonable in revised SAS simulation as compared to observation. At the same time, it is clearly seen that CFSv2 with both SAS schemes simulate the eastward and northward propagation of rainfall band reasonably well compared to TRMM observations.

The mean air temperature profile shows cold bias throughout the troposphere in both SAS schemes as compared to NCEP. The revised SAS is unable to eliminate cold temperature bias throughout the tropics as well as over ISM domain. The 850 hPa JJAS mean circulation over ISM domain is found to be realistic in revised SAS simulation but strength of the cross equatorial low level jet (LLJ) is weak as compared to NCEP but stronger compared to old SAS scheme. However, the strength of the LLJ over BoB is enhanced as compared to CFSv2 with old SAS simulation and it agrees with the observation. On the other hand, the tropical easterly jet (TEJ) at 200 hPa is captured by CFSv2 with both SAS schemes but the strength is weaker in old SAS than NCEP. However, noticeable intensification of TEJ can be seen in revised SAS simulation as compared to old SAS simulation. The tropospheric temperature (TT) is found to be underestimated throughout the tropics in both SAS schemes.

The JJAS mean convective rainfall is found to be better captured in revised SAS simulation as compared to old SAS simulation. CFSv2 with old SAS scheme considerably underestimates mean convective rainfall over Indian landmass as compared to observation. On the other hand, revised SAS simulation shows noticeable enhancement of convective rainfall over Indian landmass region as compared to TRMM 3G68. However, the convective rainfall is found to be overestimated over equatorial Pacific Ocean, equatorial Indian Ocean and west coast of Africa in CFSv2 with both SAS schemes as compared with the observation. The PDF of convective rainfall is significantly improved in revised SAS simulation over CI and it is able to reproduce proper lighter and moderate category convective rainfall as observation. On the other hand, CFSv2 with old SAS scheme considerably overestimates lighter category and underestimates moderate category convective rainfall. It is likely that the improvement in total rainfall over CI is mainly contributed by the accurate simulation of convective rainfall PDF by the revised SAS.

The simulated low cloud distributions appear to be underestimated over the eastern tropical Pacific and Atlantic oceans as compared to ISCCP estimation. However, over Indian landmass, CFSv2 with both SAS schemes

overestimate low cloud distributions. Model evaluated low cloud distribution is not realistic as compared to observation. On the other hand, both models are able to capture the spatial distribution of high cloud fractions. However, it is found that the high cloud fractions are overestimated by both SAS schemes over tropical Pacific Ocean, west coast of Africa and equatorial Indian Ocean as compared to observation. Interestingly, the high cloud fractions over Indian landmass are increased in revised SAS simulation and it agrees with the observation. Possibly, in revised SAS, the cumulus convection is stronger and deeper resulting in formation of more high clouds which causes more rainfall over Indian landmass.

From the above analysis, we have seen the remarkable impact of revised SAS in CFSv2 in simulating ISM rainfall in daily scale. However, we intend to analyze whether the daily scale rainfall improvement is coming from the sub-daily or diurnal scale? The study reveals that the revised SAS is able to capture the proper diurnal cycle and the time of rainfall maximum over CI as compared to TRMM. However, it overestimates the rainfall amount over CI. CFSv2 with old SAS scheme shows similar diurnal cycle for both the resolutions namely at T126 and T382 and is unable to reproduce the diurnal cycle in terms of magnitude as well as time of precipitation maxima. The most noticeable improvement in revised SAS in diurnal scale is found in capturing diurnal rainfall PDF over CI. The revised SAS is able to separate out the PDF of lighter and moderate category rainfall at different times of the day as compared to TRMM. On the other hand, the old SAS scheme simulates similar diurnal rainfall PDF for all the times of the day for both the resolutions. The diurnal cycle of low cloud fractions indicate that both SAS schemes are unable to capture the magnitude and peak timing. On the other hand, the revised SAS in CFSv2 is able to realistically simulate the diurnal cycle of high clouds fractions although the amplitude is underestimated.

The above analyses indicate that increase in the model horizontal resolution possibly is not the only solution to improve ISMR at different scales. There is a need to improve the physical parameterization as showed here to enhance model fidelity. Although we have seen that the rainfall has improved over ISM domain in revised SAS at T126 resolution, its implication will need to be further tested at higher resolution (T382) CFSv2. However, many other parameters such as TT, low cloud fraction etc., do not show much improvement in revised SAS simulation which essentially leaves lots of scope for future model development.

References

Abhik S, Mukhopadhyay P, Goswami BN (2014) Evaluation of mean and intraseasonal variability of Indian summer monsoon simulation in ECHAM5: identification of possible source of bias. Clim Dyn 43:389–406. doi:10.1007/s00382-013-1824-7

Abhilash S, Sahai AK, Pattnaik S, Goswami BN, Kumar A (2014) Extended range prediction of active-break spells of Indian summer monsoon rainfall using an ensemble prediction system in NCEP climate forecast system. Int J Climatol 34:98–113. doi:10.1002/joc.3668

Ajayamohan RS, Boualem Khouider, Majda AJ (2014) Simulation of monsoon intraseasonal oscillations in a coarse resolution aqua-planet GCM. Geophys Res Let. doi:10.1002/2014GL060662

Dirmeyer PA et al (2010) Simulating the hydrologic diurnal cycle in global climate models: resolution versus parameterization. Center for Ocean–Land–Atmosphere Studies Tech. Rep. 304

Barker HW, Stephens GL, Fu Q (1999) The sensitivity of domain averaged solar fluxes to assumptions about cloud geometry. Q J R Meteorol Soc 125:2127–2152

Betts AK, Jakob C (2002) Evaluation of the diurnal cycle of precipitation, surface thermodynamics, and surface fluxes in the ECMWF model using LBA data. J Geophys Res 107:8045. doi:10.1029/2001JD000427

Chattopadhyay R, Goswami BN, Sahai AK, Fraedrich K (2009) Role of stratiform rainfall in modifying the northward propagation of monsoon intraseasonal oscillation. J Geophys Res 114:1–15. doi:10.1029/2009JD011869

Chaudhari HS, Shinde MA, Oh JH (2010) Understanding of anomalous Indian summer monsoon rainfall of 2002 and 1994. Quat Int 213:20–32

Chaudhari HS, Pokhrel S, Saha SK, Dhakate A, Yadav RK, Salunke K, Mahapatra S, Sabeerali CT, Rao AS (2013) Model biases in long coupled runs of NCEP CFS in the context of Indian summer monsoon. Int J Climatol 33:1057–1069. doi:10.1002/joc.3489

Collins WD (2001) Parameterization of generalized cloud overlap for radiative calculations in general circulation models. J Atmos Sci 58:3224–3242

Dai A (2006) Precipitation characteristics in eighteen coupled climate models. J Clim 19:4605–4630

Dai AF, Trenberth KE (2004) The diurnal cycle and its depiction in the community climate system model. J Clim 17:930–995

Duchon CE (1979) Lanczos filtering in one and two dimensions. J Appl Meteorol 18:1016–1022

Ek MB, Mitchell KE, Lin Y, Rogers E, Grunmann P, Koren V, Gayno G, Tarplay JD (2003) Implementation of Noah land surface model advances in the National Centers for Environmental Prediction operational mesoscale Eta model. J Geophys Res 108(D22):8851. doi:10.1029/2002JD003296

Fennessy MJ, Kinter JL III, Kirtman B, Marx L, Nigam S, Schneider E, Shukla J, Straus D, Vernekar A, Xue X, Zhou J (1994)

The simulated Indian monsoon: a GCM sensitivity study. J Clim 7:33–43

Findlater J (1969) A major low-level air current near the Indian Ocean during the northern summer. Q J R Meteorol Soc 95:362–380

Gadgil S (2003) The Indian monsoon and its variability. Ann Rev Earth Planet Sci 31:429–467

Gadgil S, Gadgil S (2006) The Indian monsoon, GDP and agriculture. Econ Polit Wkly XLI:4887–4895

Gadgil S, Sajani S (1998) Monsoon precipitation in the AMIP runs. Clim Dyn 14:659–689

Gates WL, Boyle J, Covey C, Dease C, Doutriaux C, Drach R, Fiorino M, Gleckler P, Hnilo J, Marlais S, Phillips T, Potter G, Santer BD, Sperber KR, Taylor K, Williams D (1999) An overview of the results of the Atmospheric Model Intercomparison Project (AMIP I). Bull Am Meteor Soc 80:29–55

Goswami BN (1998) Inter-annual variations of Indian summer monsoon in a GCM: external conditions versus internal feedbacks. J Clim 11:501–522

Goswami BN (2005) South Asian summer monsoon. In: Lau WK-M, Waliser DE (eds) Intraseasonal variability of the atmosphere ocean climate system. Springer, Berlin, pp 19–61

Goswami BN, Xavier PK (2005) Dynamics of internal interannual variability of the Indian summer monsoon in a GCM. J Geophys Res 110:D24104. doi:10.1029/2005JD006042

Goswami BB, Mukhopadhyay P, Khairoutdinov M, Goswami BN (2013) Simulation of Indian summer monsoon intraseasonal oscillations in a superparameterized coupled climate model: need to improve the embedded cloud resolving model. Clim Dyn 41:1497–1507. doi:10.1007/s00382-012-1563-1

Goswami BB, Deshpande MS, Mukhopadhyay P, Saha SK, Rao AS, Murthugudde R, Goswami BN (2014) Simulation of monsoon intraseasonal variability in NCEP CFSv2 and its role on systematic bias. Clim Dyn 1–21. doi:10.1007/s00382-014-2089-5

Griffies SM, Harrison MJ, Pacanowski RC, Rosati A (2004) A technical guide to MOM4,GFDL ocean group technical report 5, GFDL, pp 337

Hack JJ, Keihl JT, Hurrell JW (1998) The hydrologic and thermodynamic characteristic of the NCAR CCM3. J Clim 11:1179–1206

Haddad ZS, Short DA, Durden SL, Im E, Hensley S, Grable MB, Black RA (1997a) A new parametrization of the rain drop size distribution. IEEE Trans Geosci Remote Sens 35:532–539. doi:10.1109/36.581961

Haddad ZS, Smith EA, Kummerow CD, Iguchi T, Farrar MR, Durden SL, Alves M, Olson WS (1997b) The TRMM 'day-1' radar/radiometer combined rain-profiling algorithm. J Meteorol Soc Jpn 75:799–809

Han J, Pan H-L (2011) Revision of convection and vertical diffusion schemes in the NCEP global forecast system. Wea Forecast 26:520–533. doi:10.1175/WAF-D-10-05038.1

Hong SY, Pan HL (1998) Convective trigger function for a mass flux cumulus parameterization scheme. Mon Wea Rev 126:2599–2620

Houze RAJ (1989) Observed structure of mesoscale convective systems and implications for large-scale heating. Q J R Meteorol Soc 115:425–461

Hoyos CD, Webster PJ (2007) The role of intraseasonal variability in the nature of Asian monsoon precipitation. J Clim 20(17):4402–4424

Huffman GJ, Adler RF, Bolvin DT, Gu G, Nelkin EJ, Bowman KP, Stocker EF, Wolff DB (2007) The TRMM multisatellite precipitation analysis: quasi-global, multi-year, combined-sensor precipitation estimates at fine scale. J Hydrometeorol 8:33–55

Iguchi T, Kozu T, Meneghini R, Awaka J, Okamoto K (2000) Rain profiling algorithm for the TRMM precipitation radar. J Appl Meteorol 39:2038–2052

Inness PM, Slingo JM, Woolnough SJ, Neale RB, Pope VD (2001) Organization of tropical convection in a GCM with varying vertical resolution; implications for the simulation of the Madden–Julian oscillation. Clim Dyn 17:777–793. doi:10.1007/s003820000148

Kalnay E, Kanamitsu M, Kistler R, Collins W, Deaven D, Gandin L, Iredell M, Saha S, White G, Woollen J, Zhu Y, Chelliah M, Ebisuzaki W, Higgins W, Janowiak J, Mo KC, Ropelewski C, Wang J, Leetma A, Reynolds R, Jenne R, Joseph D (1996) The NCEP/NCAR 40-year reanalysis project. Bull Am Meteorol Soc 77:437–471. doi:10.1175/1520-0477(1996)077<0437:TNYRP>2.0.CO;2

Kang I-S, Jin K, Wang B, Lau K-M, Shukla J, Krishnamurthy V, Schubert S, Wailser D, Stern W, Kitoh A, Meehl G, Kanamitsu G, Galin V, Satyan V, Park C-K, Liu Y (2002) Intercomparison of the climatological variations of Asian summer monsoon precipitation simulated by 10 GCMs. Clim Dyn 19:383–395. doi:10.1007/s00382-002-0245-9

Kemball-Cook S, Wang B, Fu X (2002) Simulation of the intraseasonal oscillation in the ECHAM-4 model: the impact of coupling with an ocean model. J Atmos Sci 59:1433–1453. doi:10.1175/1520-0469(2002)059<1433:SOTIOI>2.0.CO;2

Kim H-M, Kang I-S, Wang B, Lee J-Y (2008) Interannual variations of the boreal summer intraseasonal variability predicted by ten atmosphere–ocean coupled models. Clim Dyn 30:485–496. doi:10.1007/s00382-007-0292-3

Kim H-M, Webster PJ, Curry JA (2012) Seasonal prediction skill of ECMWF system 4 and NCEP CFSv2 retrospective forecast for the Northern Hemisphere Winter. Clim Dyn 39:2957–2973. doi:10.1007/s00382-012-1364-6

Kripalani RH, Kulkarni A, Sabade SS, Khandekar ML (2003) Indian monsoon variability in a global warming scenario. Nat Hazards 29:189–206

Krishna Kumar K (2005) Advancing dynamical prediction of Indian monsoon rainfall. Geophys Res Lett 32:L08704. doi:10.1029/2004GL021979

Kug J-S, Kang I-S, Choi D-H (2008) Seasonal climate predictability with tier-one and tier-two prediction systems. Clim Dyn 31:403–416. doi:10.1007/s00382-007-0264-7

Kummerow C, Hong Y, Olson WS, Yang S, Adler RF, McCollum J, Ferraro R, Petty G, Shin DB, Wilheit TT (2001) The evolution of the Goddard profile algorithm (GPROF) for rainfall estimation from passive microwave sensors. J Appl Meteorol 40:1801–1820

Lee Drbohlav H-K, Krishnamurthy V (2010) Spatial structure, forecast errors, and predictability of the south Asian monsoon in CFS monthly retrospective forecasts. J Clim 23:4750–4769

Lee MI et al (2007) An analysis of the warm season diurnal cycle over the continental United States and northern Mexico in general circulation models. J Hydrometeor 8:344–366

Liebmann B, Smith CA (1996) Description of a complete (interpolated) outgoing longwave radiation dataset. Bull Am Meteorol Soc 77:1275–1277

Lim K, Hong S, Yoon J, Han J (2014) Simulation of the summer monsoon rainfall over East Asia using the NCEP GFS cumulus parameterization at different horizontal resolutions. Wea Forecast. doi:10.1175/WAF-D-13-00143.1

Lin J-L, Weickman KM, Kiladis GN, Mapes BE, Schubert SD, Suarez MJ, Bacmeister JT, Lee M-I (2008) Subseasonal variability associated with Asian summer monsoon simulated by 14 IPCC AR4 coupled GCMs. J Clim 21:4541–4567. doi:10.1175/2008JCLI1816.1

Mahakur M, Prabhu A, Sharma AK, Rao VR, Senroy S, Singh R, Goswami BN (2013) High-resolution outgoing longwave radiation dataset from Kalpana-1 satellite during 2004–2012. Curr Sci 105:1124–1133

Mooley DA, Parthasarathy B (1984) Fluctuations of All-India summer monsoon rainfall during 1871–1978. Clim Chang 6:287–301

Naidu CV, Krishna KM, Rao SR, Kumar OSRUB, Durgalakshmi K, Ramakrishna SSVS (2011) Variations of Indian summer monsoon rainfall induce the weakening of easterly jet stream in the warming environment? Global Planet Chang 33:1017–1032

Pan HL, Wu WS (1995) Implementing a mass flux convective parameterization package for the NMC medium-range forecast model. NMC Office Note 409

Pattanaik DR, Kumar A (2010) Prediction of summer monsoon rainfall over India using the NCEP climate forecast system. Clim Dyn 34:557–572. doi:10.1007/s00382-009-0648-y

Pattnaik S, Abhilash S, De S, Sahai AK, Phani R, Goswami BN (2013) Influence of convective parameterization on the systematic errors of Climate Forecast System (CFS) model over the Indian monsoon region from an extended range forecast perspective. Clim Dyn 41:341–365. doi:10.1007/s00382-013-1662-7

Piani C, Haerter JO, Coppola E (2010) Statistical bias correction for daily precipitation in regional climate models over Europe. Theo Appl Climatol 99:187–192

Pokhrel S, Rahaman H, Parekh A, Saha SK, Dhakate A, Chaudhari HS, Gairola RM (2012) Evaporation-precipitation variability over Indian Ocean and its assessment in NCEP Climate Forecast System (CFSv2). Clim Dyn 39:2585–2608. doi:10.1007/s00382-012-1542-6

Qie X, Wu X, Yuan T, Bian J, Lu D (2014) Comprehensive pattern of deep convective systems over the Tibetan Plateau-South Asian monsoon region based on TRMM data. J Clim 27:6612–6626

Rajeevan M, Bhate J (2008) A high resolution daily gridded rainfall data set (1971–2005) for mesoscale meteorological studies. National Climate Centre Research Report (9)

Rossow WB, Schiffer RA (1999) Advances in Understanding Clouds from ISCCP. Bull Am Meteor Soc 80:2261–2287

Rossow WB, Zhang YC (1995) Calculation of surface and top of atmosphere radiative fluxes from physical quantities based on ISCCP data sets, 2. Validation and first results. J Geophys Res 100:1167–1197

Sabeerali CT, Rao AS, Ajayamohan RS, Murtugudde R (2012) On the relationship between Indian summer monsoon withdrawal and Indo-Pacific SST anomalies before and after 1976/1977 climate shift. Clim Dyn 39:841–859. doi:10.1007/s00382-011-1269-9

Sabre M, Hodges K, Laval K, Polcher J, Désalmand F (2000) Simulation of monsoon disturbances in the LMD GCM. Mon Wea Rev 128:3752–3771

Saha S et al (2010) The NCEP climate forecast system reanalysis. Bull Am Meteor Soc 91:1015–1057

Saha S, Moorthi S, Wu X, Wang J, Nadiga S, Tripp P, Behringer D, Hou Y-T, Chuang H-Y, Iredell M, Ek M, Meng J, Yang R, Pena Mendez M, van den Dool H, Zhang Q, Wang W, Chen M, Becker E (2013) The NCEP climate forecast system version 2. J Clim. doi:10.1175/JCLI-D-12-00823.1

Saha SK, Pokhrel S, Chaudhari HS, Dhakate A, Shewale S, Sabeerali CT, Salunke K, Hazra A, Mahapatra S, Rao AS (2014) Improved simulation of Indian summer monsoon in latest NCEP climate forecast system free run. Int J Climatol 34:1628–1641. doi:10.1002/joc.3791

Sahai AK, Abhilash S, Chattopadhyay R, Borah N, Joseph S, Sharmila S, Rajeevan M (2014) High-resolution operational monsoon forecasts: an objective assessment. Clim Dyn 1–12. doi:10.1007/s00382-014-2210-9

Schiffer RA, Rossow WB (1983) The international satellite cloud climatology project (ISCCP): the first project of the world climate research programme. Bull Am Meteor Soc 64:779–784

Sharmila S, Pillai SA, Joseph S, Roxy M, Krishna RPM, Chattopadhyay R, Abhilash S, Sahai AK, Goswami BN (2013) Role of ocean-atmosphere interaction on northward propagation of Indian summer monsoon intra-seasonal oscillations (MISO). Clim Dyn 41:1651–1669. doi:10.1007/s00382-013-1854-1

Slingo JM, Sperber KR, Boyle JS, Ceron J-P, Dix M, Dugas B, Ebisuzaki W, Fyfe J, Gregory D, Gueremy J-F, Hack J, Harzallah A,

Inness P, Kitoh A, Lau WK-M, McAvaney B, Madden R, Matthews A, Palmer TN, Parkas C-K, Randall D, Renno N (1996) Intraseasonal oscillations in 15 atmospheric general circulation models: results from an AMIP diagnostic subproject. Clim Dyn 12:325–357. doi:10.1007/BF00231106

Sperber KR, Annamalai H (2008) Coupled model simulations of boreal summer intraseasonal (30–50 day) variability, Part 1: systematic errors and caution on use of metrics. Clim Dyn 31:345–372. doi:10.1007/s00382-008-0367-9

Sperber KR, Palmer TN (1996) Inter-annual tropical rainfall variability in general circulation model simulations associated with the atmospheric model inter-comparison project. J Clim 9:2727–2750

Suhas E, Neena JM, Goswami BN (2013) An Indian monsoon intraseasonal oscillations (MISO) index for real time monitoring and forecast verification. Clim Dyn 40:2605–2616. doi:10.1007/s00382-012-1462-5

Ueda H, Yasunari T (1998) Role of warming over the Tibetan Plateau in early onset of the summer monsoon over the Bay of Bengal and the South China Sea. J Meteorol Soc Jpn 76:1–12

Waliser DE (2006) Intraseasonal variability. In: Wang B (ed) The Asian monsoon, 1st edn. Springer Praxis Books, Berlin, pp 203–257

Waliser DE, Jin K, Kang I-S, Stern WF, Schubert SD, Wu MLC, Lau K-M, Lee M-I, Krishnamurthy V, Kitoh A, Meehl GA, Galin VY, Satyan V, Mandke SK, Wu G, Liu Y, Park C-K (2003) AGCM simulations of intraseasonal variability associated with the Asian summer monsoon. Clim Dyn 21:423–446. doi:10.1007/s00382-003-0337-1

Wang B, Kang I-S, Lee J-Y (2004) Ensemble simulations of Asian-Australian monsoon variability by 11 AGCMs. J Clim 17:803–818. doi:10.1175/1520-0442(2004)017<0803:ESOAMV>2.0.CO;2

Wang B, Ding Q, Fu X, Kang I-S, Jin K, Shukla J, Doblas-Reyes F (2005) Fundamental challenge in simulation and prediction of summer monsoon rainfall. Geophys Res Lett. doi:10.1029/2005GL022734

Wang B, Lee J-Y, Kang I-S, Shukla J, Kug J-S, Kumar A, Schemm J, Luo J-J, Yamagata T, Park C-K (2008) How accurately do coupled climate models predict the leading modes of Asian-Australian monsoon interannual variability? Clim Dyn 30:605–619. doi:10.1007/s00382-007-0310-5

Webster PJ, Magana VO, Palmer TN, Shukla J, Tomas RA, Yanai M, Yasunari T (1998) Monsoons: processes, predictability and the prospectus for prediction. J Geophys Res 103:14451–14510

Wu X, Liang X, Zhang GJ (2003) Seasonal migration of ITCZ precipitation across the equator: why Can't GCMs simulate it. Geophys Res Lett 30. doi:10.1029/2003GL017198

Xavier PK, Marzin C, Goswami BN (2007) An objective definition of the Indian summer monsoon season and a new perspective on the ENSO-monsoon relationship. Q J R Meteorol Soc 133:749–764

Xiouhua F, Lee J-Y, Wang B, Wang W, Vitart V (2013) Intraseasonal forecasting of the Asian summer monsoon in Four operational and research models. J Clim 26:4186–4203. doi:10.1175/JCLI-D-12-00252.1

Yanai M, Esbensen S, Chu J-H (1973) Determination of bulk properties of tropical cloud clusters from large-scale heat and moisture budgets. J Atmos Sci 30:611–627. doi:10.1175/1520-0469(1973)030<0611:DOBPOT>2.0.CO;2

Yang S, Smith EA (2006) Mechanisms for diurnal variability of global tropical rainfall observed from TRMM. J Clim 19:5190–5226

Yang S, Zhang Z, Kousky VE, Higgins RW, Yoo S-H, Liang J, Fan Y (2008) Simulations and seasonal prediction of the Asian summer monsoon in the NCEP climate forecast system. J Clim 21:3755–3775. doi:10.1175/2008JCLI1961.1

Yoo H, Li Z, Hou Y-T, Lord S, Weng F, Barker HW (2013) Diagnosis and testing of low-level cloud parameterizations for the NCEP/GFS model using satellite and ground-based measurements 41:1595–1613

Zhang GJ, Mu M (2005) Simulation of the Madden–Julian oscillation in the NCAR CCM3 using a revised Zhang–McFarlane convection parameterization scheme. J Clim 18:4046–4064. doi:10.1175/JCLI3508.1

Zhang C, Dong M, Gualdi S, Hendon HH, Maloney ED, Marshall A, Sperber KR, Wang W (2006) Simulations of the Madden-Julian oscillation in four pairs of coupled and uncoupled global models. Clim Dyn 27:573–592. doi:10.1007/s00382-006-0148-2

Zhao Q, Carr FH (1997) A prognostic cloud scheme for operational NWP models. Mon Wea Rev 125:1931–1953